TU/e EINDHOVEN UNIVERSITY OF TECHNOLOGY

Optimization of Electric Ethylene Production

Citation for published version (APA):
Tiggeloven, J. L., Faaij, A. P. C., Kramer, G. J., & Gazzani, M. (2023). Optimization of Electric Ethylene Production: Exploring the Role of Cracker Flexibility, Batteries, and Renewable Energy Integration. *Industrial and Engineering Chemistry Research*, *62*(40), 16360-16382. https://doi.org/10.1021/acs.iecr.3c02226

Document license:
CC BY

DOI:
10.1021/acs.iecr.3c02226

Document status and date:
Published: 11/10/2023

Document Version:
Publisher's PDF, also known as Version of Record (includes final page, issue and volume numbers)

Please check the document version of this publication:

• A submitted manuscript is the version of the article upon submission and before peer-review. There can be important differences between the submitted version and the official published version of record. People interested in the research are advised to contact the author for the final version of the publication, or visit the DOI to the publisher's website.
• The final author version and the galley proof are versions of the publication after peer review.
• The final published version features the final layout of the paper including the volume, issue and page numbers.

Link to publication

General rights
Copyright and moral rights for the publications made accessible in the public portal are retained by the authors and/or other copyright owners and it is a condition of accessing publications that users recognise and abide by the legal requirements associated with these rights.

• Users may download and print one copy of any publication from the public portal for the purpose of private study or research.
• You may not further distribute the material or use it for any profit-making activity or commercial gain
• You may freely distribute the URL identifying the publication in the public portal.

If the publication is distributed under the terms of Article 25fa of the Dutch Copyright Act, indicated by the "Taverne" license above, please follow below link for the End User Agreement:

www.tue.nl/taverne

Take down policy
If you believe that this document breaches copyright please contact us at:

openaccess@tue.nl

providing details and we will investigate your claim.

Download date: 08. Feb. 2024

I&EC research
Industrial & Engineering Chemistry Research

Open Access
This article is licensed under CC-BY 4.0

pubs.acs.org/IECR
Article

Optimization of Electric Ethylene Production: Exploring the Role of Cracker Flexibility, Batteries, and Renewable Energy Integration

Julia L. Tiggeloven, André P. C. Faaij, Gert Jan Kramer, and Matteo Gazzani*

Cite This: *Ind. Eng. Chem. Res.* 2023, 62, 16360−16382

Read Online

ACCESS | Metrics & More | Article Recommendations | Supporting Information

ABSTRACT: The electrification of naphtha cracking for ethylene production could reduce the associated CO_2 emissions but would require significantly larger electricity consumption. Within this context, the flexible operation of electric crackers opens opportunities for improved integration with the future electricity system. In this work, we developed a computationally efficient mixed-integer linear programming model to investigate flexibility in electric crackers, exploring the effect of operational parameters, such as operating envelope, ramping time, and start-up/shut-down time, on costs and emissions. We optimized three electric cracker systems: two with grid electricity consumption (with/without batteries) and one with electricity supply from dedicated renewable technologies. We find that the operating envelope of the cracker has the strongest impact on cost savings, enabling up to 5.5% reduction when using flexible electricity from the grid and 58% for systems with direct coupling to renewables. Moreover, the flexible operation of electric crackers relying on the electricity grid enhances the CO_2 emission savings, achieving a 90.4% emission reduction against 54.6% of the constant operation case. Finally, we find that for direct coupling with renewables, electric crackers need to be flexible to avoid suboptimal oversizing of renewable technologies and especially unrealistic battery capacities.

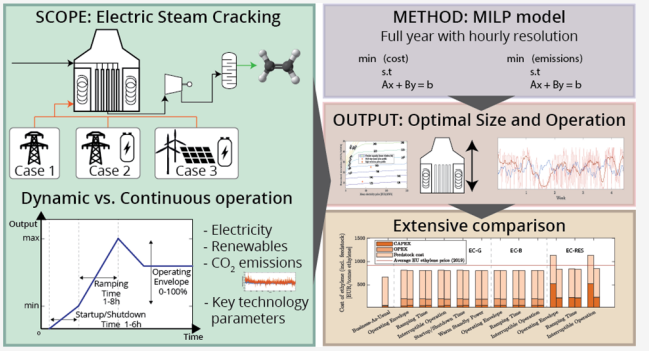

INTRODUCTION

In 2019, the industrial sector was responsible for 20 Gt of greenhouse gas emissions, representing 34% of the total global emissions.[1] While several routes exist to decrease these emissions, the industry is expected to be one of the main contributors to residual emissions in 2050.[1] For instance, achieving CO_2 neutrality within the chemical industry presents considerable challenges, to name a few: the transition to nonfossil carbon as feedstock, the complexity of redesigning synthesis processes at Mt/year scale in a limited time horizon, the use of sustainable energy, water, and land.[2] An illustrative example is the thermal cracking of hydrocarbon feedstocks for the production of light olefins, such as ethylene, which stands out among the plethora of CO_2-intensive processes in the chemical industry for the high CO_2 emissions: 300 Mt/year.[3−5] At the same time, cracking of either fossil-based or alternative feedstocks is expected to remain relevant in the future because of its capacity to deliver the requested amounts of the product while using established process technologies.

Notably, in cracking plants, around 90% of CO_2 emissions are directly related to the energy consumption of the heat provision in the steam cracker.[5] Therefore, several industrial initiatives exist that aim to electrify the process heat provision while reducing the direct emissions of ethylene production. The advantage is twofold: in electric-based heating, low-carbon electricity can be used as a heat source; moreover, the energy efficiency of the cracking process increases. However, the operation of the electric crackers could be challenging. While conventional ethylene production plants are typically operated at maximum capacity due to high investment costs and process complexity, electric crackers will inherently be exposed to fluctuating boundary conditions. At the same time, a fluctuating energy supply also presents opportunities for flexibility in operations, enabling the plant to respond to varying electricity prices that reflect the production of renewable energy production. On the one hand, the significant increase in electricity consumption due to electrification will exacerbate the role of electricity costs in overall operational expenses, leading to a new balance between investment and operating costs. On the other hand, the need to supply electricity through discontinuous renewable energy sources will require massive investments in storage capacity, lest accepting a higher risk of grid instability. By exploiting variations in electricity prices, it may be possible to lower the operating

Received: June 30, 2023
Revised: September 12, 2023
Accepted: September 12, 2023
Published: September 27, 2023

Downloaded via TU EINDHOVEN on January 26, 2024 at 09:39:34 (UTC).
See https://pubs.acs.org/sharingguidelines for options on how to legitimately share published articles.

ACS Publications
© 2023 The Authors. Published by American Chemical Society

https://doi.org/10.1021/acs.iecr.3c02226
Ind. Eng. Chem. Res. 2023, 62, 16360−16382

expenses that arise from electrification. Additionally, a flexible operation will provide a useful service to the electricity grid, facilitating the decarbonization of both the ethylene production process and the energy system as a whole.

The use of flexible operation in industry as a response to fluctuations in electricity prices, a practice commonly known as demand side management (DSM), has gained increasing attention over the past decade.[6−8] One of the main challenges in the adoption of industrial DSM, especially in the chemical industry, lies in the complexity and interdependency of the different processes; not surprisingly, conventional chemical processes are typically operated under the design conditions and possibly at a steady state. In addition to the complexity of individual processes, chemical plants are usually located in industrial clusters, where additional interactions and dependencies exist. As a result, operating industrial clusters in a flexible manner is particularly challenging.

From a simulation perspective, modeling industrial DSM can be computationally expansive: the complex nature of nonlinear formulation limits the extent to which the temporal and spatial analysis can be included. This highlights the need to develop computationally efficient formulations for modeling and optimizing industrial DSM, which can adequately capture the dynamics of chemical processes and their interactions with the energy system both inside and outside the cluster. Not surprisingly, the growing body of literature on industrial DSM adopts mixed-integer linear programming (MILP) as the state-of-the-art technique. Notably, it enables the approximation of nonlinear costs and dynamic performance of chemical processes (e.g., through piecewise linearization) and the implementation of constraints to enforce the minimum feasible operating level, ramping rates, and start-ups/shut-downs of plants. At the same time, MILP can effectively handle large-scale problems with a wide scope and high level of detail while retaining accuracy and computational efficiency.

In more detail, researchers have adopted MILP to model and assess the potential of industrial DSM in several industry types, including paper and pulp,[9−11] glass,[12] cement,[13,14] and metal.[14−17] In the chemical industry, flexible operation is analyzed for processes that typically have high electricity consumption, such as the synthesis of chlorine-based chemicals[18−20] and air separation units.[13,21−25] However, these studies simplify the problem formulation along two dimensions. First, the temporal scope is limited to a period of 1 week or less, thus neglecting seasonal fluctuations associated with renewable energy production. Second, the optimal sizing of the industrial facility is not taken into account, which means that the impact of adapting the size of the plant to lower capacity factors (i.e., flexible operation) is not fully captured. This is a crucial aspect, since implementing flexibility requires a more complex plant design and oversizing of the facility to enable the shift of production in time. These modifications result in an increase in investment costs, which can limit the savings in operating costs from exploiting electricity prices. Therefore, the trade-off between investment and operating costs needs to be evaluated, and the installed capacities of the plant, storage, and other technologies must be included as decision variables in the problem, leading to a more complex optimization. In fact, in the field of industrial DSM, only a limited number of case studies exist that optimize both the capacity and the operation of industrial processes. For instance, Miller et al.[26] conducted an economic analysis to study the impact of various boundary conditions on the flexibility of the design of an air separation unit but did not mathematically optimize the design or operation. Mitra et al.[27] optimized the operation and included the design in the analysis by considering a fixed set of plant modifications for which the operation is optimized. Other studies, such as Roh et al.,[28] introduced a sizing variable into the model, but typically had a short time horizon and used decomposition algorithms to handle the complexity of decision variables related to the plant design. To enable longer time horizons or facilitate stochastic optimization, Teichgraeber et al.[29] and Teichgraeber and Brandt[30] used time aggregation methods to cluster temporal data into representative days. Moreover, they simplify the technology models by excluding (integer) variables related to unit commitment and operation, thus resulting in a simpler yet less accurate problem formulation.

As a result, existing industrial DSM studies have not fully explored the interdependence of optimal capacity and operation variables and the benefits of flexibility under varying market conditions. Additionally, while some studies have shown that ramping constraints have little impact on the objective function but can increase computation time,[28] others have found that similar objective function values can feature different optimal design decisions.[30] This underscores the importance of accurately modeling plant operations. In summary, there is a clear research gap in the literature, with no studies that simultaneously optimize the design and operation of industrial DSM processes while still providing a full-year hourly resolution and accurately representing a plant's flexible performance. Moreover, to the best of our knowledge, no studies have investigated the adoption of DSM in electric steam crackers, which are particularly of interest due to the large electricity consumption and their role in the synthesis of platform chemicals.

This study aims to tackle this gap by applying a computationally efficient yet detailed MILP formulation to model DSM in the ethylene production process. Our approach involves optimizing the capacity and operation variables simultaneously while having a temporal scope of one year and an hourly resolution to accurately capture fluctuations in electricity prices and the underpinning availability of renewable electricity. To comprehensively explore the flexible behavior of the process while coping with the limited data available for the design of electric crackers (EC), we assess the role of three key operation parameters: the operating envelope (OE), the ramping time (RT), and the start-up and shut-down (SUSD) time, as also depicted in Figure 1. We evaluate the impact of these parameters on the cracker capacity, cost of ethylene production, CO_2 emissions, and computational efficiency and do this under varying electricity price profiles and investment costs.

Moreover, to accurately consider both the individual cracker process and its role within a larger energy system or industrial cluster, we investigate the flexible operation of EC for four different systems, as shown in Figure 2, where the portfolio of technologies varies. The first case (a) "business-as-usual" (BAU) with a conventional cracker serves as a reference for comparison. The second case (b) "electric cracker-grid" (EC-G) considers the provision of electricity from the grid exclusively. The third case (c) "electric cracker-battery" (EC-B) is connected to the electric grid but includes batteries as an alternative to the reactor's flexible operation. The last case (d) "electric cracker-renewables" (EC-RES) is independent of the electric grid and considers the sizing of renewable

https://doi.org/10.1021/acs.iecr.3c02226
Ind. Eng. Chem. Res. 2023, 62, 16360−16382

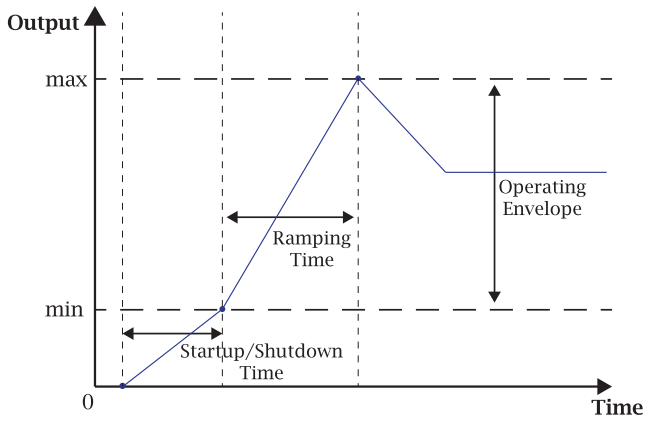

Figure 1. Example of an operational profile of a chemical plant, including the three critical operating parameters that are examined in this work: the operating envelope, the ramping time, and the start-up and shut-down time.

technologies, wind turbines and photovoltaics (PV), along with the electric cracker and batteries. In all cases, ethylene storage is included and optimally sized along with the other technologies. Finally, we investigate the system by optimizing for costs (as a baseline of the analysis) and for CO_2 emissions, which is the ultimate motivation to transit to electric crackers.

The remainder of this work is organized as follows. First, we describe the physical basis of the conventional and electric ethylene production process. Then, we explain the MILP optimization framework that is used to model and optimize the process. Finally, we show and discuss the results and present concluding remarks.

ETHYLENE PRODUCTION PROCESS: THE PHYSICAL BASES

The most common process to produce ethylene and other light olefins is the steam cracking of a hydrocarbon feedstock.[3] Although the feedstock preference is different per region (i.e., naphtha in Europe and Asia, ethane in North America and the Middle East), the primary unit operations investigated in this work are similar. This section describes the conventional and electric steam cracking processes using naphtha feedstock, based on a typical "world-scale" capacity of 1000 kt of ethylene per year.[31] Furthermore, we report the collection of performance and cost data for the processes and outline the assumptions and simplifications of this work.

Conventional Steam Cracking. A steam cracking ethylene production plant is composed of three main sections: pyrolysis (i.e., the cracker furnace and reactor), compression, and product separation. The flow sheet in Figure 3 illustrates the material and energy streams, while the corresponding mass and energy balance values are provided in Table 1.

Pyrolysis. The pyrolysis section of the conventional ethylene production plant consists of the cracker furnace, a complex piece of equipment where hydrocarbons are cracked into smaller molecules, resulting in the formation of light olefins such as ethylene. The cracker furnace is divided into two main sections: a radiant zone and a convection zone. In the radiant zone, vaporized naphtha (C01) is heated by exposing it to radiant heat from gas-fired burners, while the convection zone cools the hot flue gases from the radiant section by recovering useful heat. The convection zone is designed with multiple passes to optimize heat transfer efficiency, preheating the air and naphtha, and generating steam for use elsewhere in the production process. In this work, we adopt the energy consumption reported in the Ethylene chapter of the *Ullmann's*

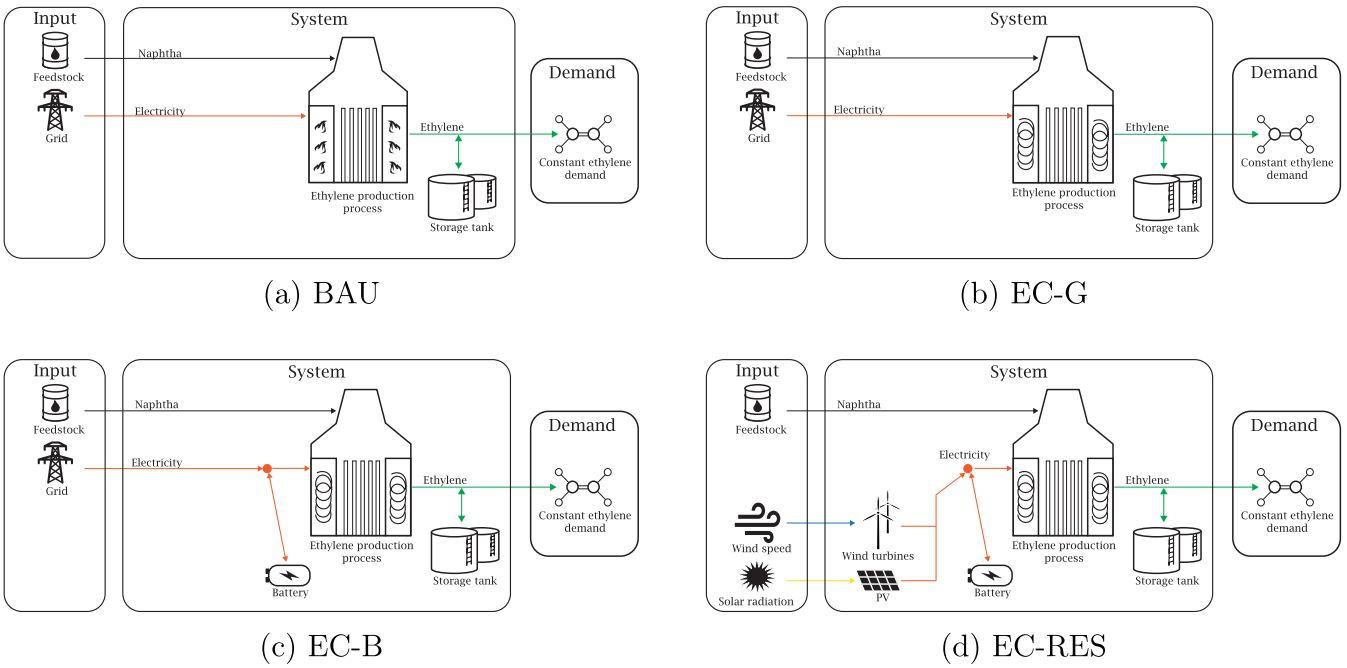

Figure 2. Schematic overview of the four systems evaluated in this work. The BAU system consists of a conventional ethylene production process and an ethylene storage tank. The EC systems replace the conventional cracker with an electric cracker. In the BAU, EC-G, and EC-B systems, electricity is consumed from the grid, and production can be shifted or electricity can be stored in a battery (only for EC-B) to exploit fluctuating electricity prices. In EC-RES, there is no grid connection and all electricity is supplied by renewables. The ethylene demand is fixed on a yearly basis for each of the four systems.

https://doi.org/10.1021/acs.iecr.3c02226
Ind. Eng. Chem. Res. 2023, 62, 16360−16382

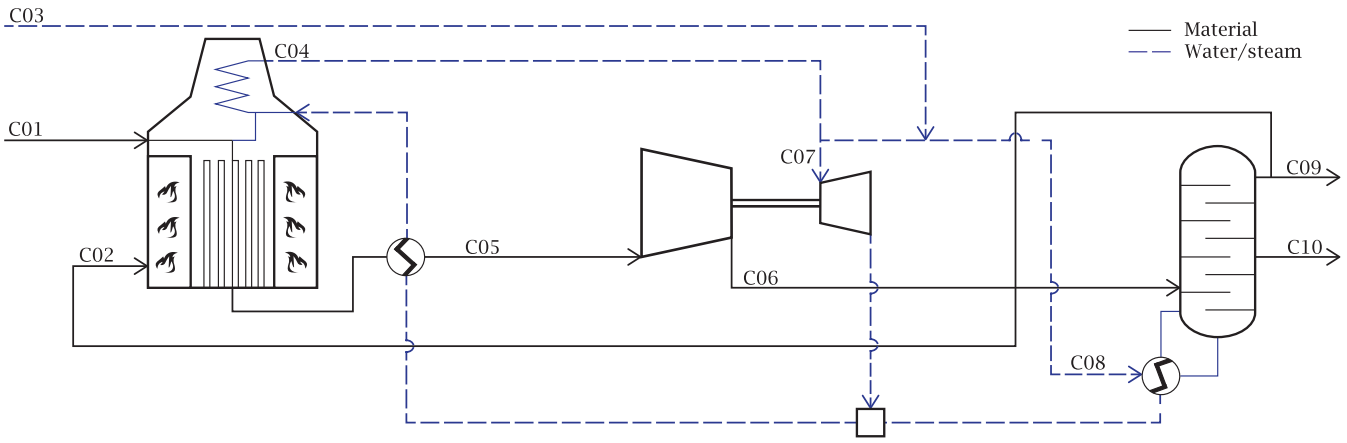

Figure 3. Overview of the energy and material streams among the cracking, compression, and separation sections of the conventional steam cracking plant. The blue arrows represent water/steam flows. The black arrows represent material flows (e.g., feedstock, fuel, and products).

Table 1. Performance Data for Each of the Three Sections of the Conventional and Electric Ethylene Production Process[a]

		conventional		electric	
section		type	value [kWh/kg naphtha]	type	value [kWh/kg naphtha]
cracker	consumption	methane	1.868	electricity	1.476
	production	superheated steam	0.841	saturated steam	0.542
compression	consumption	superheated steam	0.431	electricity	0.383
separation	consumption	saturated steam	0.492	saturated steam	0.492
	consumption	electricity	0.083	electricity	0.083
	production	methane	2.349	methane	2.349
product yield		ethylene	0.303		[kg ethylene/kg naphtha]

[a]While the electric cracker and compression sections are more energy efficient, the separation section is the same for both plants.

Encyclopedia of Industrial Chemistry (Zimmermann and Walzi), which is 1.87 kWh/kg naphtha. The value is in line with other sources, also including recent simulation works.[3,32−35] The required process heat is supplied by burning a mixture of recovered process gases (C02), with a fuel gas composition that typically consists of CH_4 and H_2 derived from the downstream separation section (for example, Spallina et al.[35] calculated 18% H_2, 81% CH_4, and 1% residues, i.e., CO and C_2H_4). Given that this gas composition is specific to the site and the configuration of the separation section (e.g., H_2 might be separated for other on-site uses), here we assume for simplicity that the fuel combusted in the furnace consists of 100% methane, leading to a small overestimation of CO_2 emissions in the conventional cracker.

At the outlet of the cracking furnace, the heat in the hot gas mixture is recovered in the transfer-line exchangers to produce high-pressure (HP) steam, which is then superheated in the convection section of the furnace. Steam production in the convection zone (C04) is calculated based on the furnace heat balance provided in Zimmermann and Walzi.[31] After heat recovery, the cracked gas is further cooled by contact with cooling oil in an oil quench tower. In a gasoline fractionator, the heavy fraction of the resulting mixture is condensed, cooled, and recycled to the oil quench tower. In some plants, the heat from oil quenching is recovered to preheat the boiler feedwater for the dilution steam that is produced in the convective section of the furnace. After separation in the primary fractionator, the cracked gas is cleaned from pollutants in a stripper.

Compression. The cooled and cleaned gas mixture (C05) is compressed in a steam turbine-driven compressor, which typically consists of four or five stages with intercooling. The energy required for compression (C07) is supplied by superheated HP steam from the cracker furnace and is here calculated according to the breakdown of energy consumption in typical naphtha steam cracking reported in Ren et al.[3] After compression, the gas mixture is dried and routed to the separation section (C06).

Separation. The separation section utilizes distillation, refrigeration, and extraction to separate products. Given the plant-specific nature of the section's design, it is assumed that the initial separation involves segregating methane from other products, which will be utilized as a combustion fuel in the furnace. Afterward, individual products are separated via multiple distillation steps, with ethylene being extracted as a liquid side stream for the purpose of storage and transport to downstream processes.[31] HP steam serves as the primary energy source for separation, while a limited amount of electricity is consumed by the cooling water, pumps, and compressors. Electricity and HP steam consumption (C08) are here calculated according to Ren et al.[3]

The energy balance of the plant yields a total specific energy consumption (SEC) of 29.1 GJ/tonne ethylene (2.44 kWh/kg naphtha) for pyrolysis and separation, which is consistent with typical values reported in the literature.[3] Similar to typical ethylene plants, the steam balance is closed via a small external gas-fired boiler (C03).[3,31] We assume the boiler consumes methane to produce HP steam with a constant efficiency of 92%,[36] regardless of the load, and a fast start-up and shut-down

https://doi.org/10.1021/acs.iecr.3c02226
Ind. Eng. Chem. Res. 2023, 62, 16360−16382

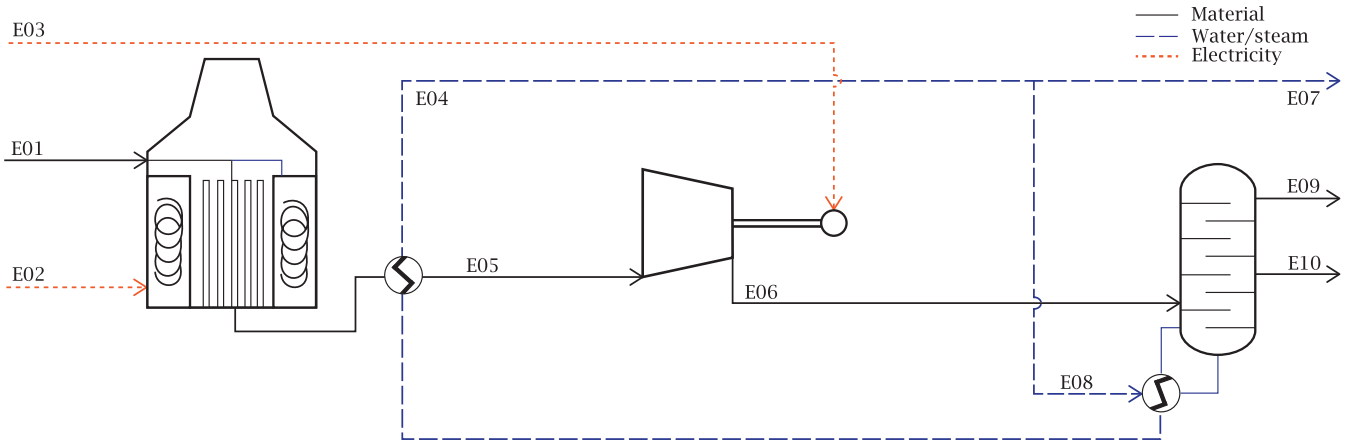

Figure 4. Overview of the energy and material streams between the cracking, compression, and separation sections of the electric steam cracking plant. The orange arrows represent electricity, the blue arrows represent water/steam flows, and the black arrows represent material flows (e.g., feedstock, fuel, and products).

time, allowing it to operate completely flexibly. The overall energy and material balance of the exemplary cracker process considered in this work are reported in Table 1.

Products. Steam cracking of naphtha yields several valuable chemicals, including ethylene, methane, propylene, toluene, and benzene. For example, high-severity naphtha cracking with a residence time of 0.4930 s results in ethylene (C10 and E10) and methane (C09 and E09) yields of 30.25 and 16.9%, respectively.[31] In the conventional process, the methane yield (C09) per kg of naphtha is higher than the fuel gas consumption (C02), and part of the methane might be exported or used in other processes. The overall balance of the different products depends on many parameters, e.g., the specific furnace and separation island design, and can vary significantly per plant. However, in this work, we are not interested in the overall, specific material output but rather in exploring a process that is capable of producing a fixed yearly amount of ethylene. Therefore, we exclusively consider the ethylene demand as a proxy of the entire cracking plant.

After separation, ethylene can be stored in a tank or directly supplied to the demand of downstream (polymer) production processes. Ethylene is stored as a liquid at a temperature between −104.5 and −90 °C and pressure between 98 and 210 kPa[37,38] in horizontal tanks (with a typical D/L = 1/4) of a maximum capacity of 350 tonnes each. Because the ethylene product is withdrawn as a liquid side stream from the separation section and typically stored for only a few hours,[31] we ignore the energy consumption required to maintain the low temperature. Furthermore, we assume that fugitive losses in the tank are negligible.

Coke Formation. The cracking of naphtha feedstock leads to coke formation inside the tubes of the pyrolysis section and in the heat-recovery section at the cracker exit, which reduces olefin selectivity.[39] An ethylene production plant, therefore, typically consists of multiple furnaces with one cracker part-time undergoing decoking and maintenance. We here consider that the nominal capacities reported in the literature account for decoking and calculate the cost and performance data accordingly. Moreover, we do not consider the decoking scheduling in the cracker operation.

CO_2 Emissions. In this work, we focus exclusively on the ethylene production process and the associated scope 1 and scope 2 CO_2 emissions, therefore neglecting the end-of-life of all exported products. While it is key for the net-zero chemical industry to consider the whole carbon cycle, scope 3 emissions are not part of this work, as they are outside the context of electric cracker capacity and operation. Moreover, we simplify scope 1 emissions by neglecting emissions from the decoking, where coke is burned with steam and air, producing CO_2. Roughly 90% of the total emissions of a conventional cracker are connected with the combustion of fuel gas in the cracker furnace to sustain the endothermic reaction (i.e., the vast majority of scope 1 emissions),[5] with the rest being mostly associated with steam boilers operation and scope 2. The resulting direct emissions of the conventional process for the cracker furnace and the boiler combined is 0.397 kg CO_2/kg naphtha, slightly higher than the value in Ren et al.[4] and in line with data from the existing crackers in The Netherlands.[40,41]

Electric Steam Cracking. The electrification of the ethylene production process represents a radical innovation that has not yet been implemented on a commercial scale. Therefore, several assumptions need to be made when considering the design and performance of an electric cracker. It is worth stressing that the detailed design of an electric cracker is not in the scope of this paper; rather, we proceeded by using available information and critical evaluation of the conventional process with respect to the new one. First, there is no reason to expect changes in the number of key sections (reactive zone, compression, separation) in an electric cracker; we therefore maintain the same division. However, significant changes take place within the first two sections: in the pyrolysis, heat is provided via electricity, and in the compression, the steam-driven compressor is substituted with electricity-driven compression. Figure 4 provides an overview of the material and energy streams among the three sections, with corresponding mass and energy balance values listed in Table 1.

Pyrolysis and Dynamic Cracker Operation. In the electric ethylene production process, indirect resistance heating is used instead of fuel combustion to preheat the air and feedstock, generate process steam, and ultimately heat and crack the vaporized naphtha (E01) into light olefins. As for conventional plants, heat is recovered from the cracked gas at the furnace outlet to produce the HP steam (E04). However, in electric cracking plants, no hot flue gas is present, therefore avoiding heat losses at the stack and removing the convective zone on

https://doi.org/10.1021/acs.iecr.3c02226
Ind. Eng. Chem. Res. 2023, 62, 16360−16382

the flue gas line; the latter was used for steam superheating in the conventional cracker, which is not required in the EC given the use of electricity-driven compressors. Overall, this results in an increased energy efficiency compared with conventional plants. Following this reasoning, we determined the energy consumption of the electric cracker (E02) based on the heat balance of the conventional furnace provided in the literature,[31] subtracting the heat for the superheating steam and the heat losses at the stack. The resulting energy consumption of an electric cracker is 21% lower than that of a gas-fired furnace.

On the other hand, the dynamic operation of electric furnaces at commercial capacities remains substantially unknown. The specific design of an electric cracker is a complex engineering task and topic of several industrial research projects.[42,43] The design of demonstration plants is strictly confidential, and only a few scientific articles discuss this. For example, Balakotaiah and Ratnakar[44] propose a novel modular reactor configuration with electrical resistance heating for endothermic reactions (i.e., steam cracking) that improves thermal efficiency (from 50 to 90%) and reduces the transient time (hours/days to seconds) compared to traditional furnace-based technologies. As the electricity consumption of the conventional process is limited, the potential for flexible operation in response to electricity prices is not of particular interest, and little research is available on operational flexibility parameters [such as the operating envelope (OE), the ramping time (RT), and the start-up and shut-down (SUSD) time]. Moreover, these industrial data are considered particularly sensitive by plant operators and technology manufacturers and therefore are not openly available. The decoking operation of a conventional cracker provides some indication of the feasible RT and SUSD time; however, as steam is used in the decoking operation, the cracker remains at a high temperature. For example, Ghashghaee and Karimzadeh[45] suggest that the feedstock flow rate can be safely ramped up/down while maintaining cracking severity (temperature), although they do not mention the impact performance and product yields for varying feedstock flow rates.

Given this context, in order to explore the impact of operational flexibility on optimal plant capacity, we focus on several key variables that can influence the integration of the ethylene production plant into the surrounding energy system including the OE, the RT, and the SUSD time. The OE is determined by the minimum feasible load point (γ) and refers to the ability of the plant to increase or decrease its steady-state production in response to changes in electricity prices or the availability of renewable electricity. The RT indicates the ability to respond quickly to external drivers and is typically determined by the time required to increase or decrease production between the minimum feasible load point and the capacity of the plant. Because we vary the OE and optimize the plant capacity in this work, we define the RT as the time required to ramp production between zero and the reference capacity, which is designed to produce 115 tonnes of ethylene per hour (around 1000 kt/year with a constant hourly production rate). The SUSD time determines how long it takes for the plant to go from shut-down to operation or vice versa, which can be important in an energy system with a significant share of renewables, as (fast) shuttling down production during times of electricity unavailability or high cost can be beneficial. Given that the OE, RT, and SUSD time of electric crackers are unknown and depend on the specific design, we run several optimizations by varying the three parameters, considering ranges that extend from nonflexible to fully flexible reactors. Additionally, we investigate the case of warm standby power (WSP), a well-known procedure in the chemical industry to enable a more flexible operation. During a warm standby, a fraction of the maximum power (ϕ) is used to maintain the tubes of the cracker at a high temperature, which prevents the thermal shock of the material due to sudden temperature fluctuations in case of fast SUSDs of the plant. An overview of the parameters and the corresponding values that are investigated in the analysis is presented in Table 2.

Table 2. Flexibility Parameters Investigated in This Work and the Corresponding Values Inserted in the Model

	unit	value
operating envelope	%	[0,20,40,60,80,100]
ramping time	h	[1,2,4,8]
start-up and shut-down time	h	[1,6]
warm standy power	%	5

Compression. Before being directed to the compressors (E05), the gas mixture undergoes cooling and cleaning processes similar to those in the conventional plant. The energy consumption of the compression section (E03) is lower than that in the conventional plant due to the higher efficiency of electric compressors, which avoids the use of steam in a mechanically driven compressor. Given that turbocompressors can move fast between different operating points (certainly faster than electric crackers), we do not consider their dynamic behavior.

Separation. The compressed gas mixture (E06) is transported to the separation section, which operates similarly to conventional plant design and results in the same electricity and steam consumption (E08). Without fuel gas consumption in the pyrolysis section and steam consumption for compression, all methane (E09) [and a marginal amount of steam (E07)] is exported or used internally, for example, to produce more ethylene via oxidative coupling of methane. In this work, we do not investigate the downstream use of fuel gas from EC, as this is out of scope. The resulting overall energy consumption for pyrolysis and separation of the electric plant is 24.4 GJ/tonne ethylene (2.05 kWh/kg naphtha).

CO_2 Emissions. The direct emissions (scope 1) of the electric plant are considered to be zero, while scope 2 emissions in EC-G and EC-B depend on the carbon intensity of the electricity grid (here investigated with different scenarios). For EC-RES, both scope 1 and scope 2 emissions are zero. As for the decoking emissions, although electrification would not completely eliminate them, the use of electric heating is expected to lead to less coke formation thanks to the more uniform temperature distribution in the tubes.[44] Therefore, we neglect decoking emissions in both conventional and electric plants.

ETHYLENE PRODUCTION PROCESS: MILP MODELING FRAMEWORK

To untangle the role of flexibility in naphtha cracking, we need a model that accurately captures the dynamic operation of the process while simultaneously maintaining computational efficiency as needed for larger energy systems optimization. Therefore, we formulate the problem via mixed-integer linear programming to optimize the capacity and operation of the

https://doi.org/10.1021/acs.iecr.3c02226
Ind. Eng. Chem. Res. 2023, 62, 16360−16382

conventional and electric plant and investigate the sensitivity of the results toward input parameters. Our model simplifies the ethylene production process for two reasons: (i) computation tractability: nonlinear formulation would add a complex set of constraints and lead to a nonlinear programming framework, thus severely limiting the number of optimization variables, and (ii) design uncertainty: having more detailed reactor models would introduce numerous assumptions (e.g., about mass and heat transfer) without adding much to the evaluation of flexibility in EC. Despite these simplifications, the model we propose can capture the essence of the ethylene production process while ensuring reasonable computational efficiency, particularly in the context of analyzing the process within a more extensive system such as an industrial cluster or region. The following section provides an overview of the optimization framework, technology models, and required input data.

Optimization Framework. The mathematical problem formulation in this work builds upon and extends the recent works of Gabrielli et al.[46,47] and Weimann et al.[48] The underpinning modeling framework is based on the energy hub approach,[49] and it has been applied to several technologies in the residential and industrial optimization domains. In the following, we provide an overview of the model, with special attention to the naphtha cracker model and with limited details on the other technologies, as they are adopted from the works mentioned above.

We model the overall ethylene production process as an industrial energy hub where several materials and energy carriers can be converted or stored and exported to satisfy the demand. The decision variables optimized by the framework include design variables (i.e., selection and size of conversion and storage technologies) and operational variables (i.e., energy and material flows and storage levels). Design and operational variables are optimized simultaneously. We use an hourly resolution, including input data about weather conditions, demand data, and prices for import and export from and to the outside of the industrial energy hub. The general formulation of the MILP is

$$\begin{aligned} \min_{\mathbf{v},\mathbf{w}} \quad & (\mathbf{c}'\mathbf{v} + \mathbf{d}'\mathbf{w}) \\ & \text{s. t.} \\ & \mathbf{A}\mathbf{v} + \mathbf{B}\mathbf{w} = \mathbf{b} \\ & \mathbf{v} \geq 0 \in \mathbb{R}^{N_v},\ \mathbf{w} \in \{0, 1\}^{N_w} \end{aligned} \tag{1}$$

where c and d are the cost vectors associated with continuous and binary decision variables v and w, respectively. A and B are the corresponding constraints, with b as the known term of the constraint, and N indicates the dimension of v and w. It can be noted that, excluding binary variables, we do not have additional generic integer variables. The problem is formulated in Matlab 2018a[50] using the YALMIP-toolbox[51] and is solved using Gurobi v9.1[52] on an Intel Xeon Silver 4110 machine (2.10 GHz, 2 sockets, 16 cores, 32 logical processors, 64 GB RAM).

Objective Functions. The reference objective function in this work is defined as the sum of the capital expenditures (CAPEX) and the operating expenditures (OPEX):

$$J = J^{\mathrm{CAPEX}} + J^{\mathrm{OPEX}} \tag{2}$$

with the annualized technology cost for the installed technologies defined as

$$J^{\mathrm{CAPEX}} = \sum_{m \in \mathcal{M}} (1 + \psi_m)(\lambda_m S_m + \zeta_m)\omega_m \tag{3}$$

where $\mathcal{M}$ is the set of available technologies in the system (described in Table 5), λ_m and ζ_m represent the size-dependent and size-independent cost parameters, and the annuity factor ω_m is used to calculate the annualized capital costs. The fixed maintenance cost of the technology is included as a fraction of annual capital costs ψ_m. The OPEX is directly determined by the energy cost of the system, given by the total amount of electricity imported, and is expressed as

$$J^{\mathrm{OPEX}} = \sum_{t=1}^{T} (\nu_{\mathrm{electricity},t} I_{\mathrm{electricity},t}) \tag{4}$$

where $I_{\mathrm{electricity},t}$ is the amount of imported electricity and $\nu_{\mathrm{electricity},t}$ is the hourly electricity price at hour t. The naphtha import cost is not included in the optimization as we assume the same ethylene yield for all plants and a constant price throughout the year (a market optimization based on the naphtha price, as, for example, done by Kwon et al.,[53] is out of the scope of the present paper).

In addition to cost optimization, we also consider an emission optimization for the electric cracker, where CO_2 emissions replace costs as the objective function. This is done as an additional analysis to investigate cracker operation when following the CO_2 intensity of the grid. More specifically, emission minimization is based on indirect emissions from imported electricity (scope 2) and is defined as

$$K = \sum_{t=1}^{T} (\varepsilon_{\mathrm{electricity},t} I_{\mathrm{electricity},t}) \tag{5}$$

where $\varepsilon_{\mathrm{electricity},t}$ are the hourly CO_2 emission factors of the electricity grid. We compare the optimized emissions of the electric cracker to those of the conventional cracker, for which we consider both grid and process emissions from the furnace.

Constraints. Several constraints are added to the problem to represent the technology characteristics, the energy and material balances, as well as auxiliary constraints needed for the practical resolution (e.g., nonnegative big-M formulations).

Energy and Material Balances. Energy and material balances are added as equality constraints for each carrier n (represented by streams in Figures 2−4) and each hour t and are formulated as follows:

$$\sum_{m \in \mathcal{M}} (I_{m,n,t} + P_{m,n,t} - F_{m,n,t}) - D_{n,t} = 0 \tag{6}$$

where $I_{m,n,t}$ is import to each technology m from outside the industrial hub, $P_{m,n,t}$ is the output of technology m, $F_{m,n,t}$ is the input of technology m from within the hub (e.g., another technology), and $D_{n,t}$ is the demand.

Performance of Generic Conversion and Storage Technologies. For each technology $m \in \mathcal{M}$ including the cracking process, the size of the technology S_m must be between a minimum and maximum value ($S^{\min}$ and $S^{\max}$):

$$S^{\min} \leq S_m \leq S^{\max} \tag{7}$$

The technology-specific operational constraints are modeled as follows:

- For the gas-fired boiler that provides the steam imbalance in the conventional plant, we adopt eqs 16 and 17 in Gabrielli et al.,[47] therefore ignoring the size-

https://doi.org/10.1021/acs.iecr.3c02226
Ind. Eng. Chem. Res. 2023, 62, 16360−16382

and load-dependent performance. Moreover, the boiler consumes methane exclusively (from the cracker fuel gas).

- The ethylene storage is modeled via eqs 18−22 in Gabrielli et al.[47] We assume no material loss, i.e., no charging and discharging efficiency.
- Batteries are modeled using eqs 18−22 in Gabrielli et al.[47] We assume the same value for charging and discharging efficiency, as they are typically similar and it simplifies the formulation.
- The offshore wind turbines are modeled via eqs 3, 4, 6, and 7 in Weimann et al.[48] As discussed in the original work, we simplify the problem assuming that continuous curtailment is possible.
- The electrical power output of a PV panel is modeled based on ambient temperature and solar irradiation as described in eq 3 in Gabrielli et al.[47]

Ethylene Production Process. The ethylene production plant is modeled as a conversion technology in which the primary input, naphtha, is converted into ethylene and methane, consuming electricity, fuel gas, and steam. The energy and mass balances are as described in the previous section for conventional and electric plants. Given that the part-load performance is not known, we assume a constant conversion efficiency from the naphtha feedstock, $F_{\text{naphta},t}$, to the final products, $P_{n',t}$, and constant energy and mass requirements (i.e., fixed relationships between input carriers are used). Accordingly, the products $P_{n',t}$ of the ethylene production plant are described as

$$P_{n',t} = \alpha_{n'} F_{\text{naphtha},t} \;\forall\, t \in T,\; n' \in \mathcal{N}' = \{\text{ethylene, methane, steam}\} \tag{8}$$

while the required inputs to the ethylene production plant $F_{n'',t}$ are computed as

$$F_{n'',t} \geq \beta_{n''} F_{\text{naphtha},t} \;\forall\, t \in T,\; n'' \in \mathcal{N}'' = \{\text{electricity, methane, steam}\} \tag{9}$$

where $\alpha_{n'}$ and $\beta_{n''}$ represent the conversion efficiency per kg of naphtha feedstock of the outputs $n' \in \mathcal{N}' \subset \mathcal{N}$ and the ratio between inputs $n'' \in \mathcal{N}'' \subset \mathcal{N}$, respectively. Note that methane and steam can be input or products depending on the specific section of the production process, e.g., input in the separation but output from the furnace.

As also shown in Figure 1, in this work, we consider and investigate three parameters that impact the plant capacity and operation in response to changes in electricity prices and renewable electricity availability: (i) the operating envelope (OE), (ii) the ramping time (RT), and (iii) the start-up and shut-down (SUSD) time.

The OE of the plant adds the following disequality constraint:

$$\gamma_{\text{naphta}} x_t S_{\text{cracker}} \leq F_{\text{naphta},t} \leq x_t S_{\text{cracker}} \;\forall\, t \in T \tag{10}$$

where $x_t \in \{0, 1\}$ represents the on/off status of the plant and γ_{naphta} is the minimum feasible operating point of the plant as a fraction of the installed capacity of the cracker, S_{cracker}. It should be noted that the constraint becomes linear when SUSDs are not allowed. The installed capacity of the plant is optimized based on its operation in response to electricity prices or availability. When flexible operation takes place, this leads to an installed capacity that is larger than the reference capacity, $S^{\text{ref}}_{\text{cracker}}$, lowering the utilization of the plant.

Next, the RT is enforced by the following disequality constraints:

$$-\frac{S^{\text{ref}}_{\text{cracker}}}{RT} \leq F_{\text{naphta},t} - F_{\text{naphta},t-1} \leq \frac{S^{\text{ref}}_{\text{cracker}}}{RT} \;\forall\, t \in T \tag{11}$$

with RT representing the time required to ramp up or down between the minimum load and the maximum capacity and $S^{\text{ref}}_{\text{cracker}}$ the size (in terms of naphtha input) of the inflexible reference plant. In this equation, we use $S^{\text{ref}}_{\text{cracker}}$ to fairly compare different values of RT, as having the decision variable S_{cracker} would imply different RT values for different design capacities.

The SUSD constraints are required to mimic the start-ups and shut-downs of plants, and their formulation is dependent on the time required to complete the transitory. In the case of interruptible operation, a set of additional constraints (based on constraints 4−6 in Morales-España et al.[54]) is required to enforce the on/off status and SUSD logic:

$$x_t - x_{t-1} = y_t - z_t \;\forall\, t \in T \tag{12}$$

$$y_t \leq x_t \;\forall\, t \in T \tag{13}$$

$$\sum_{i=t-\text{TD}+1}^{t} z_i \leq 1 - x_t \;\forall\, t \in [TD,\, T] \tag{14}$$

(12)

where the integer variables y_t and z_t represent a start-up or shut-down of the process, respectively. The minimum downtime TD is defined as the duration of a full shut-down and start-up cycle, and the minimum uptime is equal to the duration of the one time step, which is 1 h.

Depending on the specific design of the electric cracker, the SUSD times might be very long, imposing an SUSD trajectory. In this case, the operational process during on-status remains unchanged (x_t is one), following eq 10. However, an additional constraint is necessary to regulate the naphtha input and ethylene production during SUSD trajectories (if longer than the temporal resolution of the model, which is 1 h), i.e., when x_t is zero. This results in the following equality constraint:

$$(1 - x_t) F_{\text{naphtha},t} - \sum_{u=1}^{\tau} E^{\text{SUSD}} y_{(t-u+\tau+1)} - \sum_{u=1}^{\tau} E^{\text{SUSD}} z_{(t-u+1)} = 0 \;\forall\, t \in T \tag{15}$$

where τ is the duration of one start-up or shut-down. The naphtha input during start-up or shut-down periods $E^{\text{SUSD}}_{\text{naphtha}}$ is calculated by

$$E^{\text{SUSD}} = \frac{\gamma_{\text{naphtha}} S_{\text{cracker}}}{(\tau + 1)} \tag{16}$$

Finally, thermal shock of the material inside the tubes can occur during fast SUSDs, as a result of sudden temperature changes in the cracker. However, it is often possible to ramp up and down production safely (within safe RTs) as long as the temperature is maintained, as discussed in Ghashghaee and Karimzadeh[45] for conventional processes during decoking periods. Therefore, a strategy implemented in high-temperature processes to avoid thermal shock is to maintain the equipment hot while no output is produced (note, for example, that this is successfully done in fast operation of heat-recovery boilers in combined cycles). To consider this, the following

https://doi.org/10.1021/acs.iecr.3c02226
Ind. Eng. Chem. Res. 2023, 62, 16360−16382

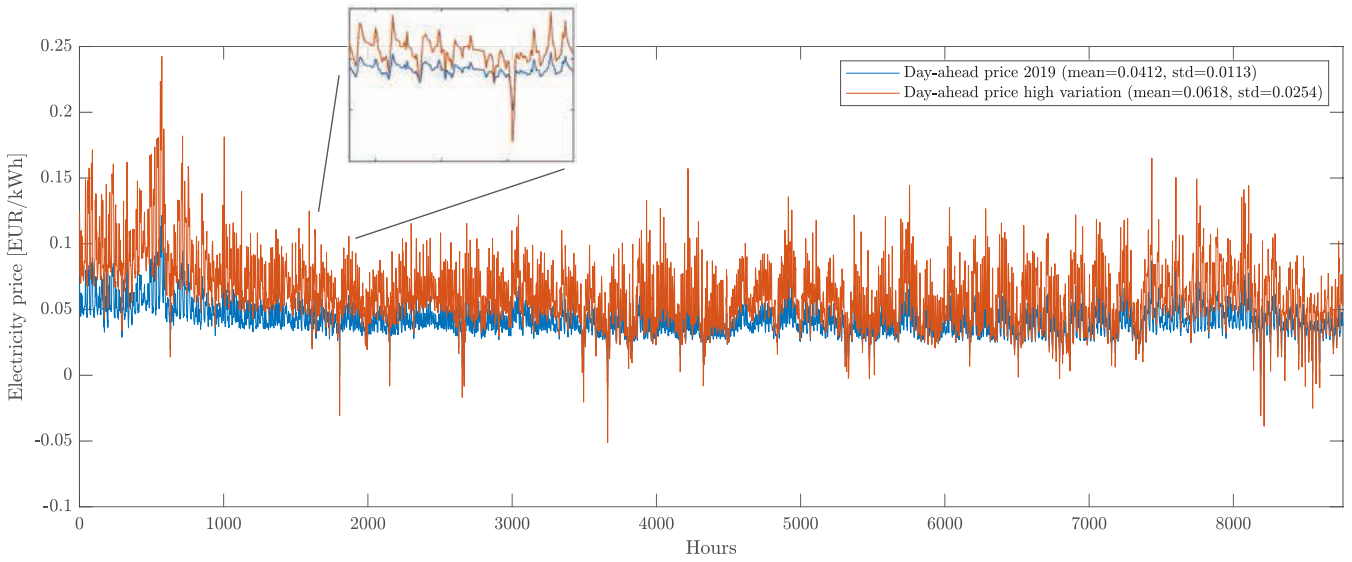

Figure 5. Day-ahead market price profile for electricity in The Netherlands for 2019 (blue) and with an increased mean and standard deviation (red).

constraint is added to the model, which represents the power needed to keep the cracker at a high temperature:

$$F_{\text{electricity},t} \geq (1 - x_t)\phi S^{\text{ref}}_{\text{electricity}} \quad \forall\, t \in T \tag{17}$$

where ϕ is a fraction (<1) of the maximum electric power of the inflexible reference plant $S^{\text{reference}}_{\text{electricity}}$.

To assess the effect of these parameters, we consider four distinct operation modes with different levels of complexity in terms of the constraints they impose:

- No start-ups and shut-downs: The plant can adjust its load within the OE, subject to the RT constraint; shut-downs are not permitted ($x_t = 1\ \forall t \in T$ in eq 10).
- Fast interruptible operation: The plant can start-up and shut-down at all times and can adjust the load within the OE, subject to the RT constraint. The SUSD time in case of fast interruptible operation is less than 1 h and the WSP is zero.
- Slow interruptible operation: Similar to fast SUSDs, the plant can start-up and shut-down at all times and can adjust the load within the OE subject to the RT constraint, and the WSP is zero. However, the SUSD time is longer than 1 h (6 h).
- Interruptible operation with warm standbys: Here, we assume a fast interruptible operation (SUSD time $\leq$ 1 h) enabled by WSP and therefore include eq 17 with an additional consumption of 5% of the electrical load for the inflexible production at $S^{\text{ref}}_{\text{cracker}}$.

The different operating modes result in different problem complexities. The absence of start-ups and shut-downs leads to the relaxation of all integer variables that enforce on/off status, resulting in a relatively straightforward implementation and resolution. Allowing for start-ups and shut-downs, however, requires the introduction of integer variables, which creates bilinearities in eq 10 and increases the model's complexity significantly via big-M formulation. The inclusion of slow start-up and shut-down trajectories requires an additional constraint (eq 15) that also involves bilinearities, further increasing the complexity. It is important to note that, as seen in eqs 10, 15, and 16, fixing the plant's capacity would eliminate these bilinearities from the formulation. However, since design and operational decision variables are interdependent, they must be optimized simultaneously.

Input Data. Our analysis of the ethylene production process aims at being location agnostic; however, depending on the specific case study depicted in Figure 2, real location-dependent data are necessary to solve the optimization, for example, with respect to ambient temperature, renewable generation, and electricity prices. Given that we do not see any advantage in using randomly generated time-series data, we retrieve baseline data from Dutch institutions and investigate their role via sensitivity analyses, e.g., on the electricity price.

Electricity Price and CO_2 Emissions. Electricity is either bought from the grid or produced within system boundaries by renewables, depending on the case study. For the cost of electricity, we utilize as a baseline the 2019 Netherlands day-ahead market price.[55] The reasonable future expectation is that the average and fluctuations in electricity prices will increase in the future due to higher demand and the integration of undispatchable renewables (large price fluctuations are already clearly visible at present during sunny days). However, substantial uncertainty in these projections remains as several location-dependent factors will drive the market development. To account for this, we analyze the system for 160 varying electricity price profiles that feature a variation in the mean and standard deviation of the original profile. The reader is referred to the Supporting Information for a more detailed description of the generation of these profiles. Two profiles (the 2019 profile and the baseline future profile) are depicted in Figure 5 with the respective mean and standard deviations.

In addition to the electricity price, we use the time-dependent CO_2 intensity of the grid for the emission minimization case study. The average CO_2 intensity of the Dutch electricity grid in 2019 was 0.369 kg CO_2/kWh, with projections of a decrease to 0.208 and 0.094 kg CO_2/kWh in 2025 and 2030, respectively.[56] The hourly CO_2 intensity profile was derived based on the hourly production of natural gas, coal, nuclear, solar, and wind in 2019 and incorporating the corresponding CO_2 emission factors from van Cappellen et al.[56] The resulting CO_2 profile has an average value of 0.372 kg

https://doi.org/10.1021/acs.iecr.3c02226
Ind. Eng. Chem. Res. 2023, 62, 16360−16382

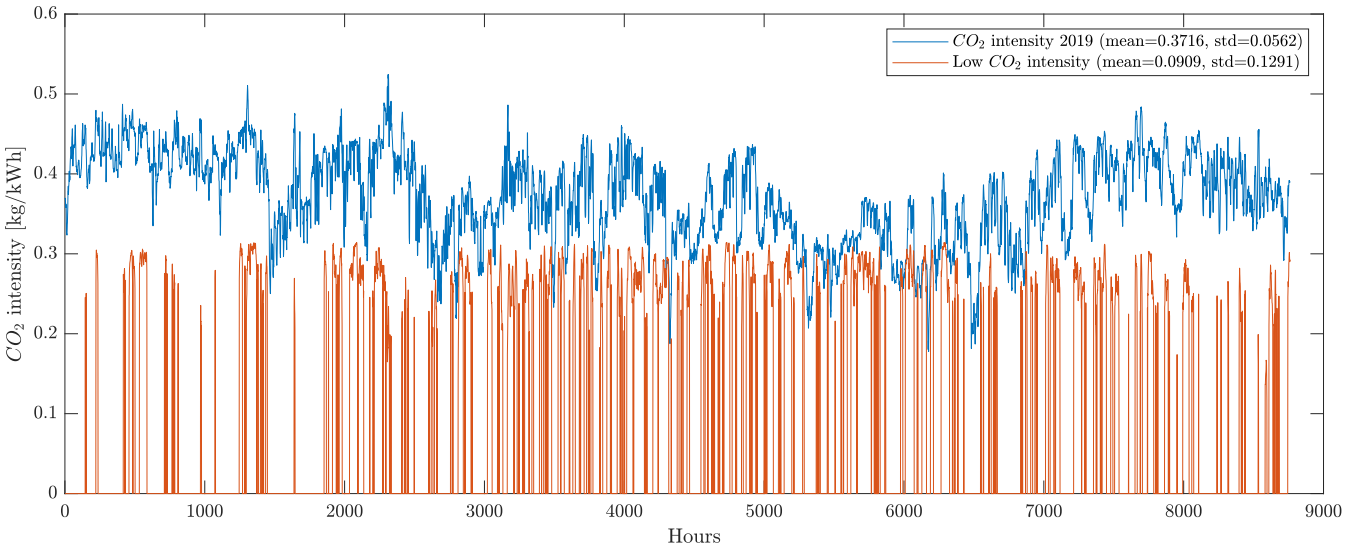

Figure 6. Hourly CO_2 intensity profiles estimated for the years 2019 (blue) and 2030 (red). The 2030 CO_2 profile and the more variable price profile in Figure 5 are completely independent.

Table 3. Cost Parameters of the Conventional Plant, the Electric Plant, and the Auxiliary Technologies

	type	unit	[€$_{2019}$/unit]	[M€$_{2019}$]	[%]	source
conventional plant	C_2H_4 production	kg_{C2H4}/h	5126.0	405	0.04	Zimmermann and Walzi[31]
electric plant	C_2H_4 production	kg_{C2H4}/h	5126.0	405	0.02	Zimmermann and Walzi[31]
gas-fired boiler	steam production	kW	72.1		0.04	DEA[36]
ethylene tank	storage	kg_{C2H4}	19.5		0.02	Turton et al.[60]
Li-ion battery	storage	kWh	168.9		0.01	DEA[62]
8.4 MW wind turbine	offshore wind	turbine	23.8×10^6		0.02	DEA[61]
ground mounted PV	PV	m^2	188.2		0.01	DEA[61]

CO_2/kWh, which aligns well with the value reported in van Cappellen et al.[56] To estimate the average CO_2 intensity of 2030, we increased renewable electricity generation, set coal-fired electricity generation to zero, and decreased gas-fired electricity generation at times of high renewable availability. This results in a CO_2 intensity profile with an average value of 0.091 kg CO_2/kWh and a renewable electricity share of 76.3%, which is consistent with the projection of van Cappellen et al.[56] The summary of the emission factors, the total annual generation for the 2019 and 2030 profiles, and a more elaborate explanation on the method used to obtain the profiles can be found in the Supporting Information and in Table S1. It should be noted that the approaches to generate the 2030 CO_2 profile and the baseline future price profile in Figure 5 are fully independent, i.e., the profiles are unrelated to each other. The coupling is out of scope, and the profiles are used in independent analyses exclusively. The hourly 2019 and 2030 CO_2 intensity profiles are depicted in Figure 6.

Weather Data. Hourly resolved solar irradiations and wind speeds are obtained from the Dutch Meteorology Institute (KNMI)[57] and the Dutch Offshore Wind Atlas (DOWA),[58] respectively, for a location near the port of Rotterdam, which could accommodate a direct connection to offshore wind parks. In this work, we ignore the cost of transmission of electricity to the onshore connection; however, it is important to note that the dedicated grid connection is vital for the electrification of ethylene production.

Technology Costs. In order to maintain consistency in the capital cost data across all technologies, we have adopted the calculation of the total overnight cost (TOC) of equipment, as outlined by the NETL.[63] The TOC is determined from the base equipment cost (BEC) through the application of the following equation:

$$\mathrm{TOC} = ((\mathrm{BEC}\cdot\mathrm{IF})\cdot\mathrm{ICF})\cdot\mathrm{COCF} \tag{18}$$

where the values of installation factor (IF), indirect cost factor (ICF), and contingencies and owner's cost factor (COCF) have been set to 1.8, 1.14, and 1.15, respectively.[35,63] For simplicity, these factors have been assumed to be consistent across all conversion and storage technologies. However, it should be noted that these values are reported based on industrial (power) plants, and therefore, the capital costs of other technologies may be inflated. Table 3 presents an overview of the cost parameters for all conversion and storage technologies.

Conventional Plant. The investment costs associated with the ethylene production process are highly dependent on the specific plant, and real data are not disclosed because of confidentiality. In fact, obtaining reliable cost numbers on complex chemical equipment is one of the biggest challenges in system modeling works. Nevertheless, capital cost estimates for typical plants have been reported by Zimmermann and Walzi,[31] Yang and You,[34] and Spallina et al.[35] In this work, we have calculated the TOC for each of the reported values via eq 18, correcting for inflation based on the year 2019 as the reference. A scaling factor of 0.6 was applied, and the resulting cost curves were used to estimate the size-dependent and size-independent cost parameters. After comparing the results, we selected the cost curve obtained from Zimmermann and Walzi,

https://doi.org/10.1021/acs.iecr.3c02226
Ind. Eng. Chem. Res. 2023, 62, 16360−16382

which is also our main source for the mass and energy balances.

Electric Plant. We assume that the capital costs for the equipment (compressors, pumps, distillation columns, etc.) in an electric cracker plant are comparable to those of a conventional cracker plant, with the exception of the cracking furnace. Moreover, we take the perspective of an *n*th-of-a-kind cracker instead of a first-of-a-kind. In other words, we do not consider the cost of the realization of the technology. Navigant Consulting[59] reports cost data for an electric furnace of 10 MW (thermal), which is used to compute cost curves using a scaling factor of 0.6. We compare the resulting cost parameters for the electric furnace with those of the conventional furnace [the conventional cracker furnace accounts for 29.5% of the plant's bare erected cost (BEC)[35]] and find that the cost difference between the two plants at a typical capacity of 1000 kt of ethylene per year is less than 1%. Therefore, the same cost parameters are used for both plants, disregarding the negligible difference. We however check the influence of this with additional sensitivity analyses.

Ethylene Storage Tank. The cost curves for the BEC of the ethylene storage tank are calculated utilizing the Capcost2017 approach described in Turton et al.,[60] with stainless steel as the chosen material of construction. Given that ethylene is produced as a liquid stream, there is no need for additional equipment to liquefy ethylene prior to storage. The TOC is determined through eq 18, taking into account inflation, and estimating the cost parameters.

Other Technologies. The cost parameters for the boiler, battery, wind turbines, and PV have been sourced from the Danish Energy Agency,[36,61,62] and it has been assumed that these costs are linear regardless of the installed capacity.

Technology Performance. The performance data of the ethylene production process is described in the previous section, specifically Table 1 for the conversion performance of energy and material carriers for both conventional and electric plants and Table 2 for the investigated values with respect to the flexibility of the electric process. In Table 4, we summarize the performance of the other conversion and storage technologies.

RESULTS

In the following, we use the model formulation and the data described above to optimize the plant capacity and operation of three different electric cracker systems (EC-G, EC-B, and EC-RES) and to compare them to the business as usual (BAU) case (as shown in Figure 2). A summary of the considered technologies per case study is reported in (Table 5). The analysis identifies not only the implications of flexible operation on the ethylene plant (EC-G and EC-B) but also the additional costs needed to balance energy supply and demand considering direct coupling to renewable energy production (EC-RES).

Table 4. Lifetime and Performance Parameters of the Auxiliary Technologies[a]

	lifetime [y]	efficiency [%]		
gas-fired boiler	25	92.0		
ground mounted PV	25	NA		
8.4 MW wind turbine	25	NA		
	lifetime [y]	loss [%]		
		charge	discharge	self-discharge
ethylene tank	15	100.0	100.0	0
Li-ion battery	15	98.0	98.0	0

[a]The performance of wind turbines and PV is determined by the weather data and modeled as described in Weimann et al.[48] and Gabrielli et al.,[47] respectively.

Table 5. Overview of the Four Systems Analyzed in This Work, Graphically Represented in Figure 2

	technologies available	electricity import
BAU	conventional cracker, ethylene tank	yes
EC-G	electric cracker, ethylene tank	yes
EC-B	electric cracker, ethylene tank, Li-ion battery	yes
EC-RES	electric cracker, ethylene tank, Li-ion battery, offshore wind, PV	no

The results are presented in two main sections: in the first, we focus on minimizing total annual costs, while in the second we focus on minimizing CO_2 emissions. It is important to note that we keep costs and emission minimization separate from each other. In both sections, we compare the inflexible electric plant to the conventional plant and analyze the potential of flexible operation of the electric cracker in both cost and emission reduction.

Cost Optimization. As a starting point, we computed the cost associated with ethylene production of the BAU and EC-G system assuming inflexible production and a reference cracker capacity of 1000 kt of ethylene per year. Even though the capital cost difference between a conventional and electric ethylene production plant is assumed to be less than 1%, the cost of ethylene production (excluding feedstock) of EC-G is 200% higher than that of the BAU for 2019 electricity prices. Moreover, when considering the higher and more variable price profile in Figure 5, this cost difference increases to almost 300%. This is the result of high electricity consumption in the EC-G system. Specifically, the import costs of electric cracking account for 70.6% of the total annual costs in the EC-G system compared to 9.2% in the BAU.

The low share of electricity costs of the conventional plant makes flexible operation in response to electricity prices irrelevant. However, since electricity import is the main driver of the excessive costs in electric cracking, allowing for flexible operation in response to fluctuating electricity prices can lead to significant cost savings. By solving a simplified model of the EC-G system, relaxing the constraint in eq 10 (i.e., the OE is 100% and x_t is always 1), and excluding the constraints in eqs 11−17, we obtain an upper limit of the costs savings that can be achieved when operating an electric ethylene production process fully flexibly. We find that the total annual cost savings when simultaneously optimizing the capacity and operation of the electric plant are 0.4 and 5.5% compared to the inflexible plant for the 2019 price profile and the future baseline price profile, respectively. It is worth stressing that these cost savings would quickly reduce were the size not optimally selected; for example, the 5.5% savings would decrease to 2.6% when using the optimal size obtained with the 2019 price profile for the future profile case. This highlights the importance of optimizing the capacity simultaneously with the operation, especially for higher and more variable electricity prices.

Next, we examined the sensitivity of the costs of ethylene production toward electricity prices and CAPEX. Given the uncertain nature of future electricity prices, we optimized the

https://doi.org/10.1021/acs.iecr.3c02226
Ind. Eng. Chem. Res. 2023, 62, 16360−16382

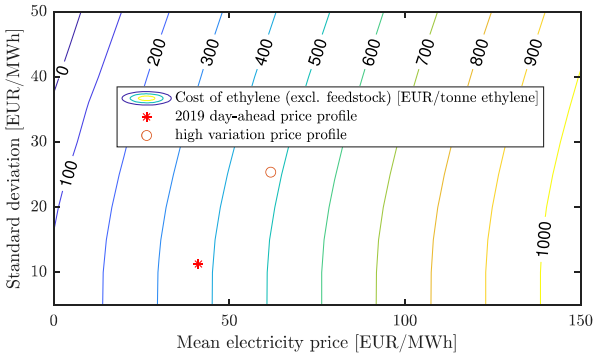

(a) Cost of ethylene production (excl. feedstock) for a size-independent cost fraction of 41%, λ_m=5126 €/(tonne C_2H_4/h) and ζ_m=405 M€.

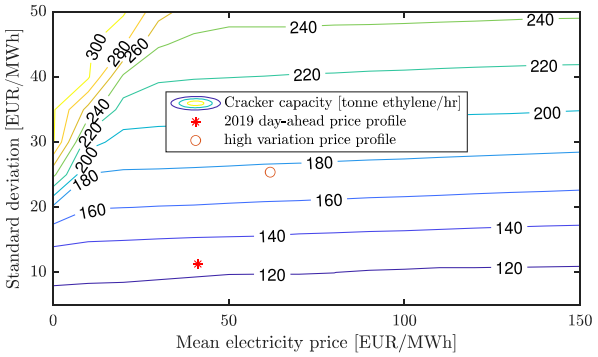

(b) Optimal installed cracker capacity for a size-independent cost fraction of 41%, λ_m=5126 €/(tonne C_2H_4/h) and ζ_m=405 M€.

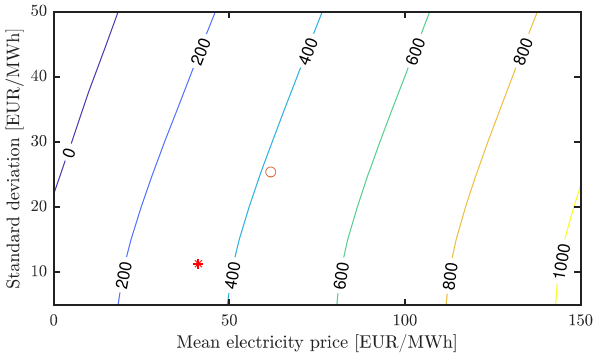

(c) Cost of ethylene production (excl. feedstock) for a size-independent cost fraction of 77%, λ_m=2050 €/(tonne C_2H_4/h) and ζ_m=769 M€.

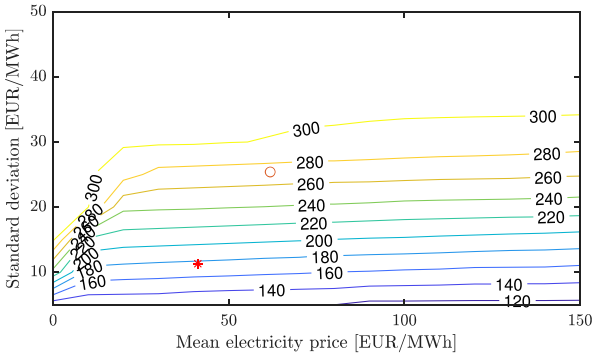

(d) Optimal installed cracker capacity for a size-independent cost fraction of 77%, λ_m=2050 €/(tonne C_2H_4/h) and ζ_m=769 M€.

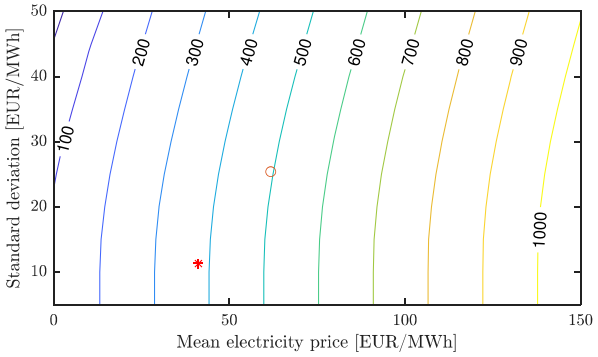

(e) Cost of ethylene production (excl. feedstock) for a size-independent cost fraction of 18%, λ_m=7177 €/(tonne C_2H_4/h) and ζ_m=182 M€.

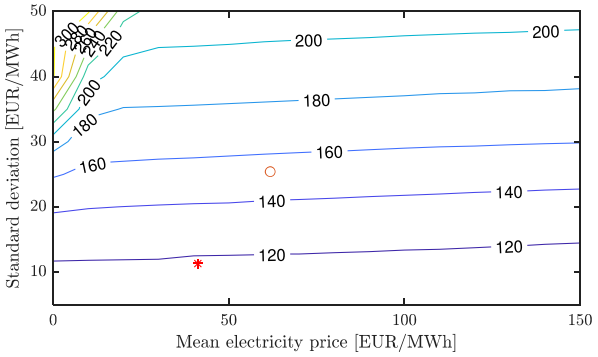

(f) Optimal installed cracker capacity for a size-independent cost fraction of 18%, λ_m=7177 €/(tonne C_2H_4/h) and ζ_m=182 M€.

Figure 7. Sensitivity analysis for the EC-G system of the cost of ethylene production and the optimal cracker capacity toward the mean and standard deviation of the hourly electricity price. (c–f) Analysis of the sensitivity for an increased or decreased size-independent fraction in the total investment cost. The reference capacity of 1000 kt ethylene annually is equal to 115 tons per hour. For comparison, the cost of ethylene production via the BAU case according to our simulations is 123 €/ton C_2H_4 excluding feedstock.

flexible operation and capacities of the EC-G system for 160 electricity price profiles with varying combinations of mean and standard deviation. In addition, we changed the structure of the CAPEX by varying the plant's size-dependent and size-independent cost parameters, λ_m and ζ_m. The analysis is carried out at a fixed yearly demand of ethylene; therefore, more flexibility means larger cracker size and lower capacity factors. The results in terms of ethylene production costs and optimal cracker capacity are depicted in Figure 7. More specifically, Figure 7a,b shows the ethylene production cost and optimal cracker capacity for the baseline λ_m and ζ_m, while Figure 7c–f shows the same at higher or lower, respectively, size-independent cost fraction of the total investment cost at reference capacity. When looking at the baseline figures for cost and size (a,b), the analysis reveals that the cost of ethylene production is mostly defined by the mean electricity price,

https://doi.org/10.1021/acs.iecr.3c02226
Ind. Eng. Chem. Res. 2023, 62, 16360−16382

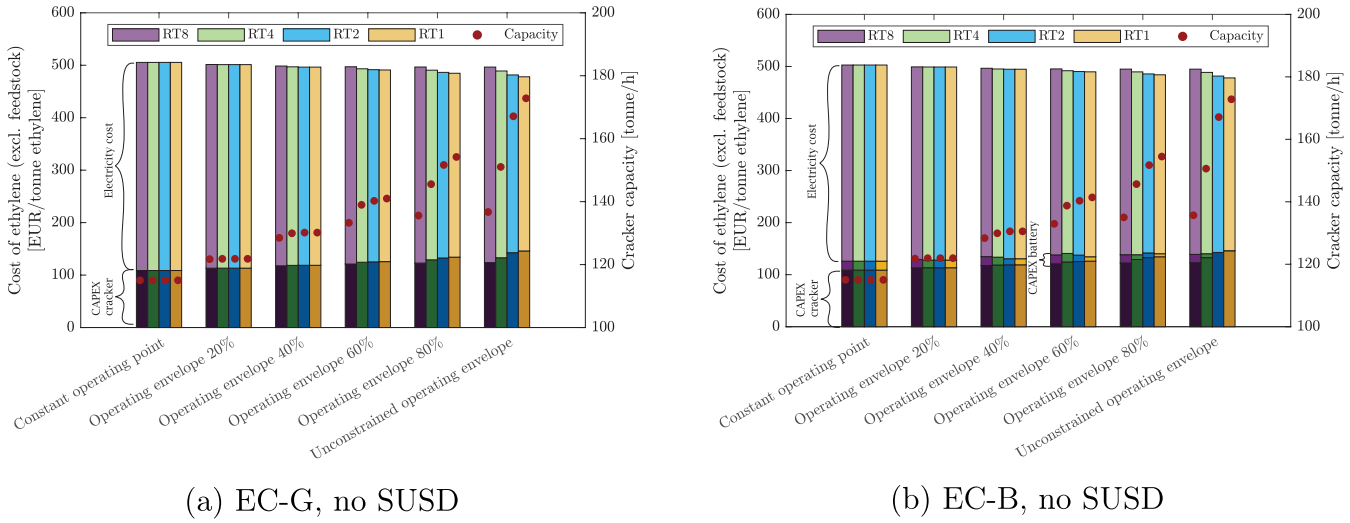

(a) EC-G, no SUSD (b) EC-B, no SUSD

Figure 8. Costs of ethylene production (excluding feedstock) and cracker capacities of the noninterruptible operation mode for varying OEs and RTs, with increasing flexibility from left to right. The different shades from light to dark represent import cost, battery capital cost (EC-B only), and ethylene plant capital cost.

while the optimal size is mostly affected by the standard deviation (except for price profiles with relatively low means and high standard deviations). Notably, different price profiles can lead to similar ethylene production costs only if the size is optimally selected, where the change in optimal size is significant (e.g., from 120 to 300 $t_{C_2H_6}$/h). The isoline cost curves bend slightly with the standard deviation, indicating a relatively lower production cost for the same mean electricity price at a higher standard deviation. As expected, the bending is stronger for a low mean electricity price. Figure 7c shows that the role of standard deviation is stronger for a higher size-independent cost fraction as the cost of installing an additional unit of capacity is relatively low while allowing for significant OPEX savings. The optimal installed cracker capacity is still predominantly determined by the standard deviation, and the maximum size is reached at a lower standard deviation. For a lower size-independent cost fraction, as depicted in Figure 7f, the trend is very similar to that in the baseline cases.

No Start-Ups and Shut-Downs. The analysis to date has considered a completely flexible electric cracker, therefore establishing a theoretical upper limit of cost savings. However, this will likely not be physically possible, and we need to explore the effects of considering the practical limitations of such an operation. In the operating mode discussed here, it is assumed that the production process cannot be interrupted, but it is still capable of adjusting its production within the specified operational range, subject to the restriction imposed by the RT constraint (eq 11). Figure 8 shows the associated cost of ethylene production and cracker capacity for different OEs and RTs in the case of electricity imported from the grid with and without a battery (EC-G in Figure 8a and EC-B in Figure 8b). The values depicted exclude the cost of naphtha and the value of byproducts. The corresponding installed capacities and simulation times of all technologies for the three EC systems can be found in Supporting Information Tables S2 and S5, respectively.

It can be noted that the cost differences of producing ethylene for varying levels of operational flexibility are minimal for both EC-G and EC-B, which is consistent with the established 5.5% upper limit of cost savings. The maximum cost savings between RT (τ) 1 and 8 h in the plant with unconstrained operation is 3.7%. However, the system designs for different degrees of operational flexibility feature significant variations in cracker and ethylene storage capacities. For example, the cost-optimal flexible capacity is over 50% larger than the inflexible capacity. Notably, differences in system design between EC-G and EC-B are negligible, except for the battery capacity, which implies that the electricity storage is only used to exploit prices to a further extent than the plant is able to. Consequently, in a completely flexible system with fast RTs and a wide OE, no electricity storage is installed. In less flexible systems, adding electricity storage leads to a maximum cost savings of only 0.5%, while a battery capacity of almost 780 MWh is required. This is a consequence of the inherently large size that batteries must possess to play a role in the cracking process.

The limited potential for cost savings, despite the notable differences in system design, is due to the trade-off between the investment and operating costs. To achieve electricity cost savings through flexible operation while having a constant ethylene demand, additional capacity must be installed, resulting in higher investment costs. Whether cost savings are achieved through flexible operation is dependent on factors such as electricity prices and size-related cost parameters, which introduce a high degree of uncertainty. As a result, investing in flexible process design when responding to electricity prices presents a significant risk, which may anyhow be required depending on other boundary conditions (e.g., grid stability).

The results from EC-G and EC-B present the system from a traditional industrial operator's perspective, assuming continuous electricity availability and responding to electricity prices. In reality, the flexibility of operation also influences optimal capacities beyond the plant's battery limits, particularly with the incorporation of substantial amounts of renewable electricity. To meet the continuous demand of the industrial sector, investments must be made elsewhere in the energy system to balance supply fluctuations. This is evident in our EC-RES results, shown in Figure 9, as the cost of ethylene production for a fully flexible EC is 57.9% lower compared to

https://doi.org/10.1021/acs.iecr.3c02226
Ind. Eng. Chem. Res. 2023, 62, 16360−16382

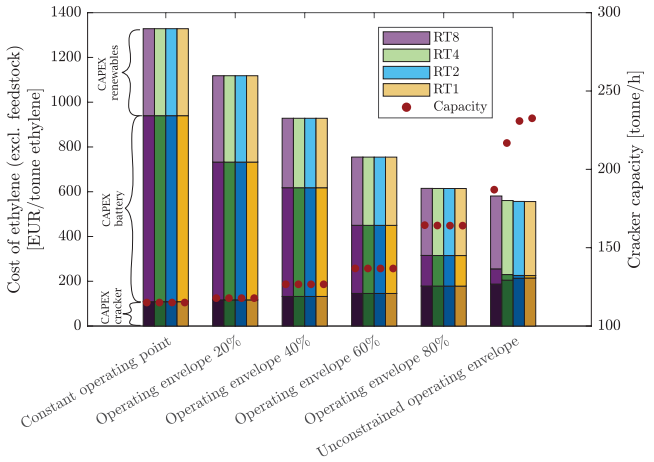

Figure 9. EC-RES costs of ethylene production (excluding feedstock) and cracker capacities of the noninterruptible operation mode for varying OEs and RTs, with increasing flexibility from left to right. The different shades from light to dark represent renewables, battery, and ethylene plant capital costs.

that for an inflexible EC. The cost decrease for varying RTs is again minimal, at a maximum of 4.2%.

A clear advantage of flexible cracker operation is the reduction in the required installed capacity for renewable electricity, which is expected to remain a limiting factor in the near future. Specifically, the decrease in the required offshore wind and photovoltaic capacity is 14.8 and 71.3%, respectively, between an inflexible cracker operation and a cracker with an unconstrained OE. Additionally, the battery capacity decreases from an unrealistic 37.4 GWh to a more sound 500 MWh. Although it is unlikely that such a large buffer capacity will be provided solely by batteries, this demonstrates the need for a buffer to meet the continuous industrial demand. Notably, when using a fully flexible cracker, the ethylene production cost increases by only 16.7% when including the capital cost of renewables (comparing EC-G with EC-RES), meaning that with this additional investment, the heat provision of the ethylene production process can be fully decarbonized. For inflexible operations, this cost difference rises to 148%. In conclusion, while the potential of flexible operation from an operator's perspective may seem limited, a wider perspective highlights the value of providing flexibility in processes that rely heavily on renewable electricity.

In addition to analyzing the optimal capacity of installed technologies, we examine the operation of the cracker (Figure 10) and storage behavior (Figure 11) for the EC-G and EC-B scenarios. Similar profiles for the EC-B case can be found in Supporting Information Figures S2 and S3. The profiles distinctly illustrate the hourly and seasonal variations as a result of fluctuating electricity prices and the availability of renewable power. This underscores the significance of adopting a comprehensive yearly and hourly temporal resolution within the optimization framework. While the full-year profile of the EC-G scenario suggests little fluctuations in plant operations, a close inspection reveals daily and weekly variations that are clearly visible in the first month and hourly profiles. The EC-RES results indicate that responding to the availability of renewables leads to seasonal variations, as visible in the optimal

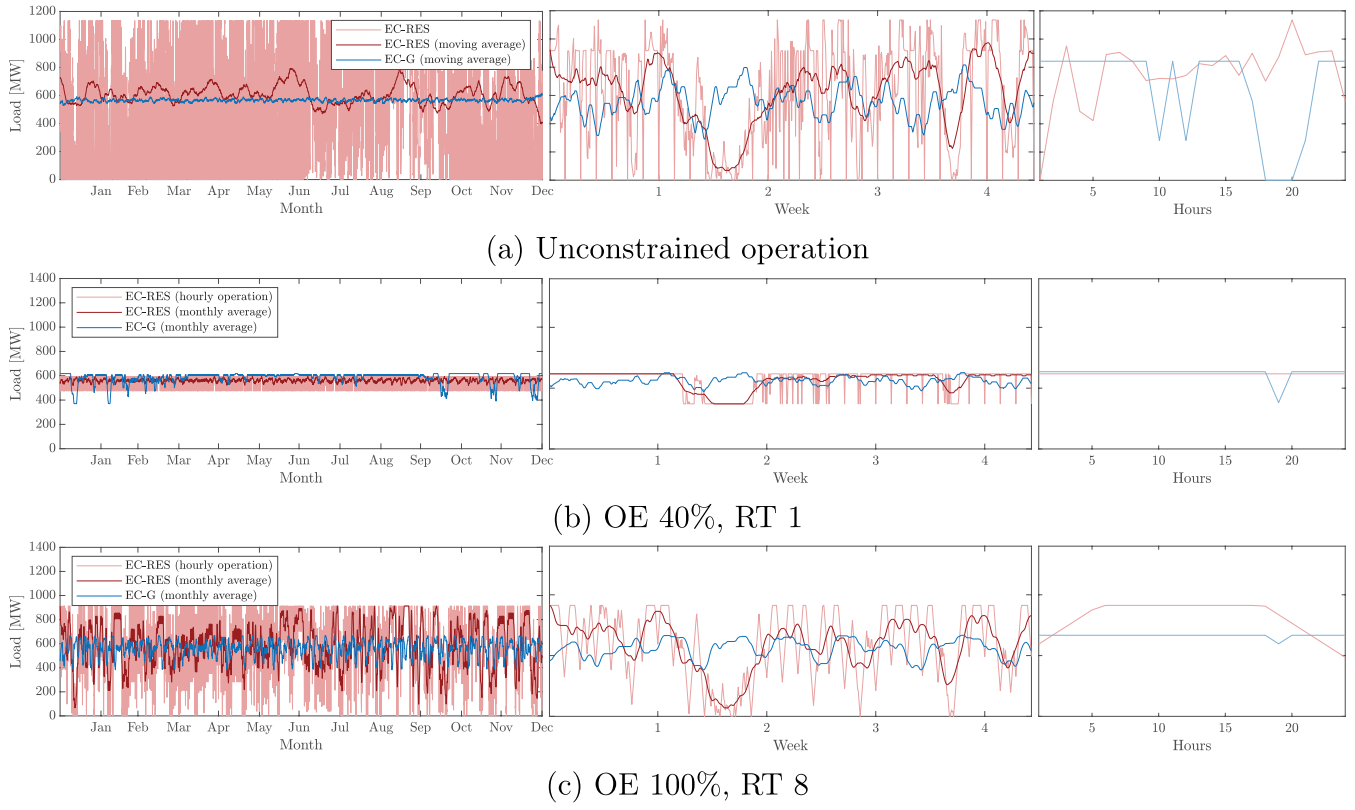

Figure 10. EC-G (blue) and EC-RES (red) cracker operation profiles of the full year, the first month, and the first day of the second week (left to right) for the noninterruptible operation mode and varying OEs and RTs. The darker blue and red lines in the full year and first month of operation represent the moving averages of the EC-G and EC-RES cases, respectively.

https://doi.org/10.1021/acs.iecr.3c02226
Ind. Eng. Chem. Res. 2023, 62, 16360−16382

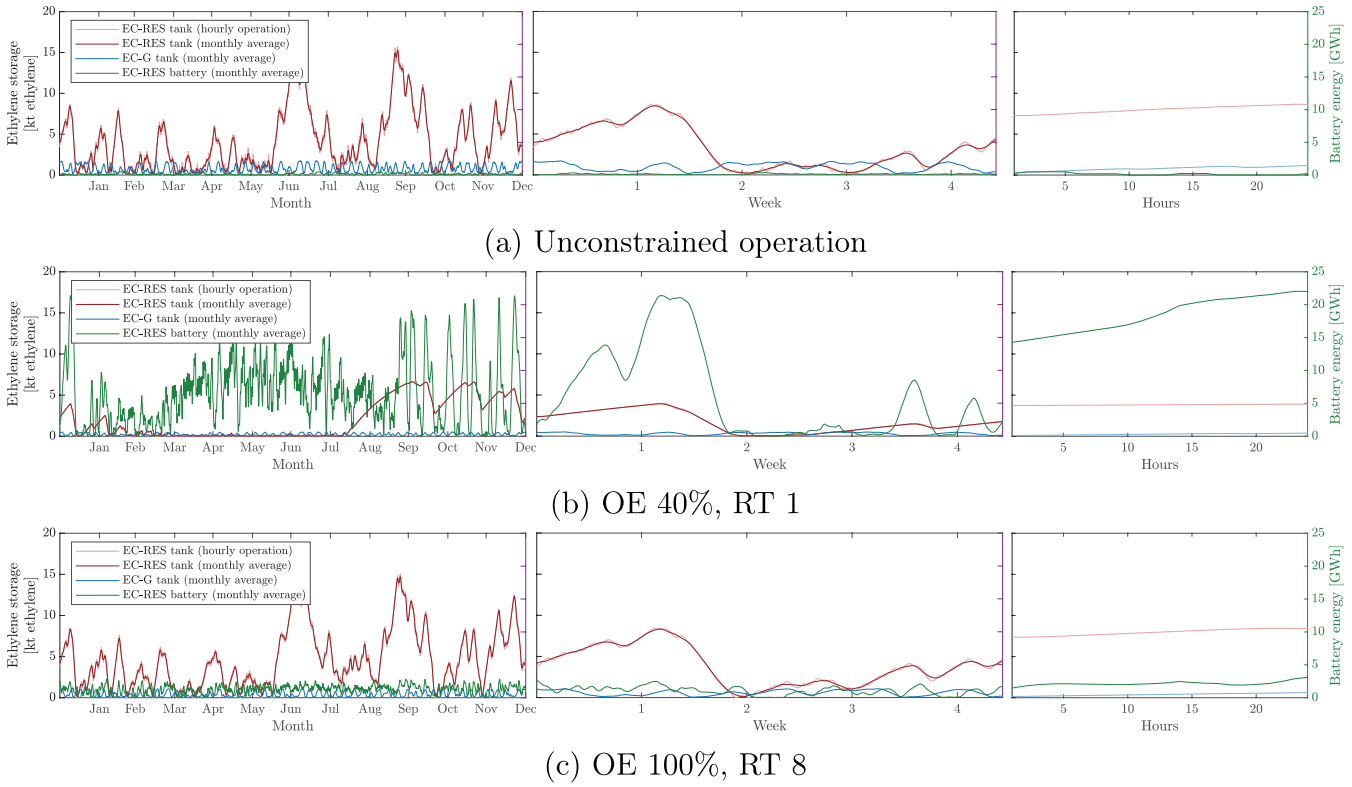

Figure 11. Battery operation for the EC-RES system (green) and ethylene storage operation for the EC-G (blue) and EC-RES (red) systems of the full year, the first month, and the first day of the second week (left to right) for the noninterruptible operation mode and varying OEs and RTs. The darker green, blue, and red lines in the full year and first month of operation represent the moving averages of the EC-G and EC-RES cases, respectively.

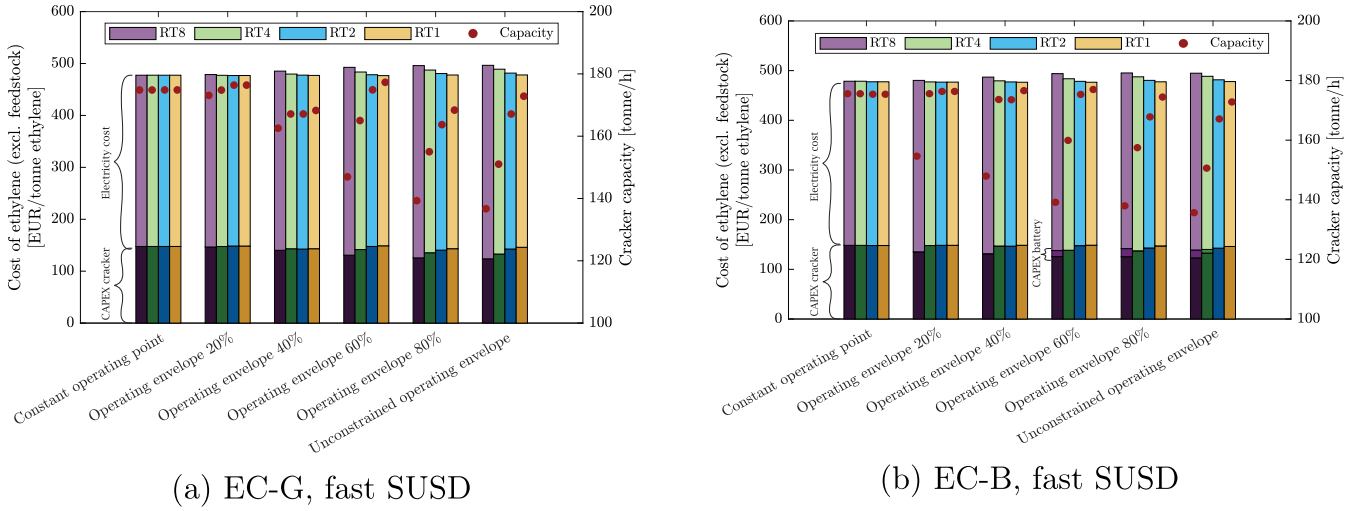

Figure 12. Costs of ethylene production (excluding feedstock) and cracker capacities of the interruptible operation mode for varying OEs and RTs, with increasing flexibility from left to right. The different shades from light to dark represent the import cost, battery capital cost (EC-B only), and ethylene plant capital cost.

operation depicted in Figure 10a, where the plant's electrical load of the plant surges during summer months due to the higher availability of renewable electricity. This increased ethylene production results in two prominent peaks in the product inventory in June and September, evident in Figure 11a. As a result, inflexible production with direct renewable coupling requires long-term buffer capacity, with battery capacities in the order of several GWh in the case of small OEs. It is therefore clear that similar combinations will be hardly feasible, thus calling for flexibility in the electrification of large industrial processes. Furthermore, we observe the impact of constraining the OE and RT on the overall system operation. Limiting the OE to 40% (Figures 10b and 11b) induces a significant change in cracker operation, especially in the EC-RES results, which leads to the significant cost differences depicted in Figure 9. Due to the lower cracker flexibility, the two summer peaks in ethylene storage utilization in the unconstrained operation are replaced by employing a

https://doi.org/10.1021/acs.iecr.3c02226
Ind. Eng. Chem. Res. 2023, 62, 16360−16382

larger battery capacity to bridge the gap between renewable electricity supply and the electricity demand of the cracker process. On the other hand, limiting the RT to 8 (Figures 10c and 11c) yields an hourly operation profile deviating from the optimal yet yielding similar monthly averages, thereby explaining the marginal influence on ethylene production costs. The three EC-G profiles in Figure 10 exhibit very similar patterns, consistent with the modest cost differences in Figure 8a.

Regarding the computational complexity and impact of constraints in this operation mode, it is worth noting that the simulations for the three different plant configurations (EC-G, EC-B, EC-RES) were solved to optimality [with a 0.1−0.5% Mixed-Integer Programming (MIP) gap] within a maximum time of approximately 30 min. Nevertheless, the computation time increases significantly with longer ramping times (τ), which is in line with the findings reported by Roh et al.[28]

Fast Interruptible Operation. Next, we investigate how rapid temporary interruptions would affect the performance and the capacity, where rapid start-ups and shut-downs take less than 1 h. The evaluation of the system design and cost of ethylene production follows the same two-stage approach as before, focusing first on variability in electricity prices (EC-G and EC-B) and second on the availability of renewables (EC-RES). The results of this analysis, in terms of ethylene production cost and cracker capacity for varying OE and RT scenarios of EC-G and EC-B, are depicted in Figure 12a−b, respectively. The corresponding installed capacities of all other technologies and the simulation times for the three EC systems can be found in Tables S3 and S5 of the Supporting Information.

When fast interruptible production is possible, operational flexibility can be increased by temporarily discontinuing the process, for example during periods of high electricity prices. As a result, the ethylene production cost decreases (e.g., −4.8% for constant operating point production in EC-G), and larger plant capacities are optimal. The difference between interruptible operation and operation without SUSDs is particularly visible for simulations with smaller OEs (i.e., <80%), as systems with large OEs are already relatively flexible in the operation. Moreover, we find that the OE becomes less important for the system design and performance compared to the noninterruptible operation mode while the RT has a similar effect on the system. Note, however, that RTs and SUSD times are typically inherently connected, as it is hard to imagine a reactor that can shut-down/start-up fast (<1 h) while having multihour RTs. This might however be achieved with specific operation strategies, such as the warm standbys that we analyze later. Finally, comparing the EC-G and EC-B results, we find that negligible additional flexibility benefits are achieved through the deployment of batteries, as it results in a cost reduction within the MIP gap.

As expected, the computational burden of constraints for interruptible operations is significantly larger than for non-interruptible operations. This is primarily due to the introduction of additional integer variables. When the OE is small or the RT is slow, operational decision variables are highly interconnected and result in a limited set of feasible solutions that can be explained via integer constraints. Notably, a close-to-optimal design for complex systems with fast interruptible operation can be found to relax the system to a linear version.

The increased complexity of the problem becomes particularly challenging for the EC-RES system, where renewable technologies must be optimized (capacity and operation) along with the cracker. In fact, it was impossible to solve the problem within 15 h under standard optimization settings for RTs longer than 1 h. Therefore, given that previous results indicated that varying RTs do not significantly affect the objective and system capacities, we optimized the EC-RES system at different OEs but for RT1 (τ = 1) exclusively. Also, in this case, the resolution was possible only by restricting the variables' range and using previous optimal results as a guideline. The results for EC-RES are listed in Figure 13.

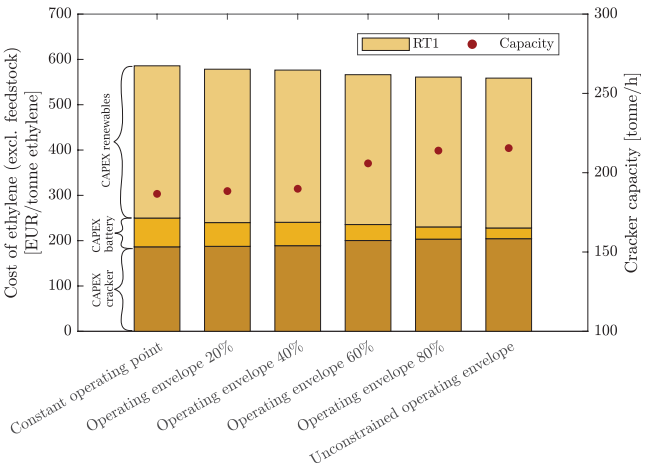

Figure 13. EC-RES costs of ethylene production (excluding feedstock) and cracker capacities of the interruptible operation mode for varying OEs. The flexibility increases from left to right and the RT is equal to the length of the one time step (1 h). The different shades from light to dark represent renewables, battery, and ethylene plant capital costs.

The results indicate that implementing fast interruptible operation in ECs when responding to renewable electricity availability can lead to a significant reduction in the cost of ethylene production, as compared with operating the plant without start-ups and shut-downs. The additional capital cost of dedicated renewable generation (the EC-RES system) is limited to an increase of 16−22% compared with the EC-G system. By contrast, for noninterruptible operations, this cost increase varies from 16 to 150%. The cost difference between interruptible and noninterruptible operation can be primarily attributed to the reduced need for battery capacity to stabilize fluctuations in renewable electricity generation, as the plant can now suspend production during periods of low availability. The greatest cost savings are observed in scenarios with small OE, where allowing for shut-downs can significantly enhance the plant's ability to respond to electricity supply fluctuations. The findings therefore call for a modular cracker design, where such fast SUSDs can be practically implemented.

Warm Standbys. The practical implementation of the fast interruptable operation mode in chemical plants with high processing temperatures presents several challenges. A warm standby, in which the cracker is kept at a high temperature through electric heating, could facilitate a fast interruptible operation. We here assess the impact of including the WSP on the optimization results of EC-G for an RT (τ) of 1. The optimization results show that the differences in objective function with and without WSP are negligible, i.e., less than the

https://doi.org/10.1021/acs.iecr.3c02226
Ind. Eng. Chem. Res. 2023, 62, 16360−16382

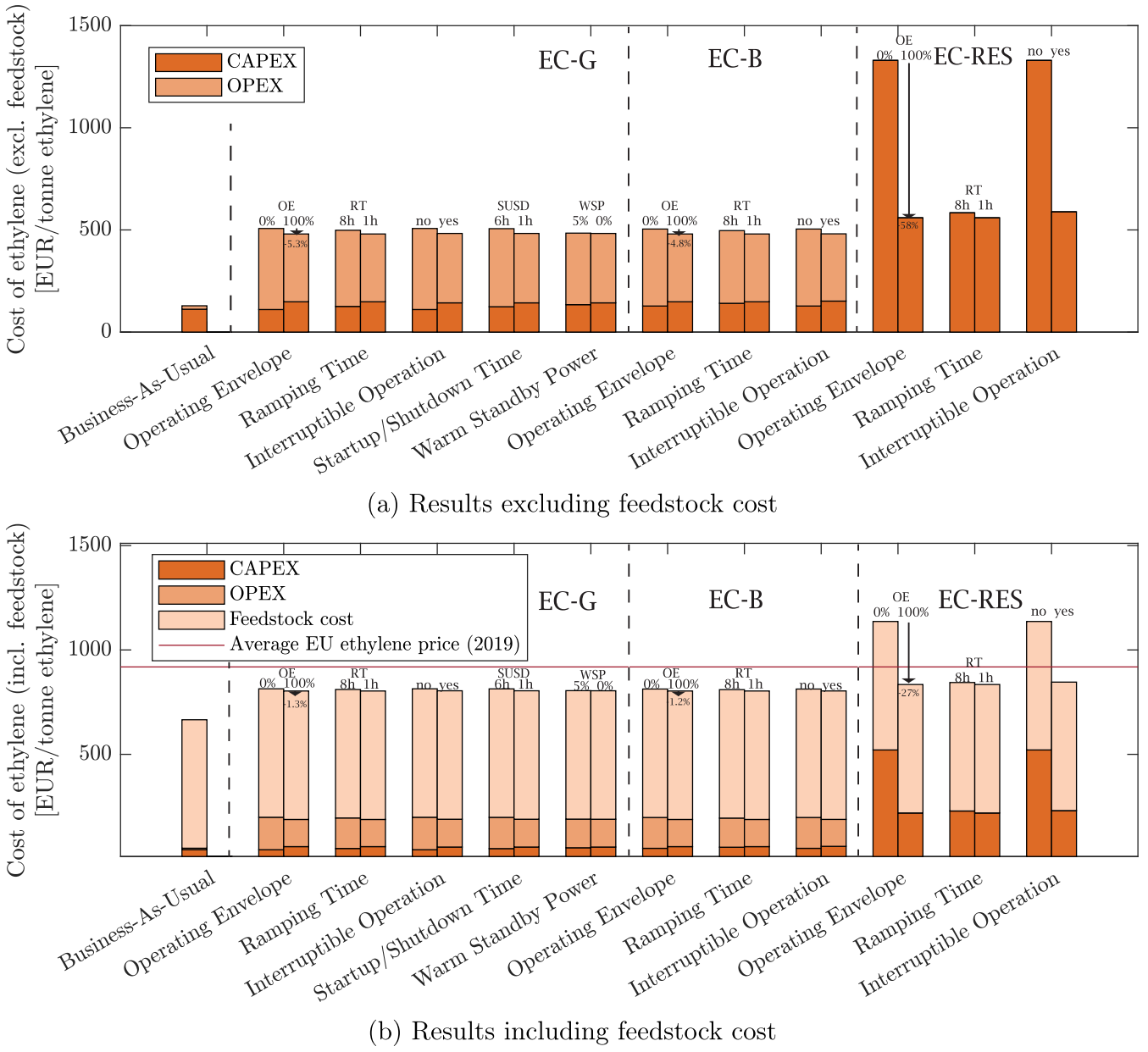

Figure 14. Overview of the cost of ethylene production (excluding and including feedstock cost) for the two extreme instances of the three investigated systems and operating parameters. The maximum ethylene production cost savings for each system are indicated with an arrow and the red horizontal line represents the average European ethylene price in 2019.[66]

MIP gap. Moreover, the differences in cracker capacities are also limited: with the inclusion of the WSP, a decrease in cracker capacity of 2−6% is obtained for OEs larger than 80%. In conclusion, if warm standbys can technically enable fast interruptible operation, it allows for the practical implementation of flexibility in the cracker while resulting in a minor increase in electricity consumption and changes in system costs and design. Therefore, under these conditions and assumptions, the benefits of a fast interruptible operation outweigh the costs of increased electricity consumption. From a modeling perspective, this operation mode can provide a more accurate formulation to model interruptible operation without adding complexity (the WSP constraints did not lead to longer computation times).

Slow Start-Ups and Shut-Downs. Another practical complication associated with fast interruptible operation is the rapid ramping up or down of production during start-ups or shut-downs, which can exceed safe limits. This is particularly problematic for small OEs, as in those cases a start-up or shut-down may require the production to be ramped up from zero to the minimum feasible operating point (or vice versa) within 1 h. In this final analysis, we explore the system operation when the SUSD time is 6 h. This significantly increases the complexity of the model formulation, as discussed in the previous section.

Despite the additional complexity of the constraints, we conducted a sensitivity analysis on EC-G cases, providing a comprehensive evaluation of the system performance. Our results indicate that the difference in objective between fast and slow SUSDs is at most 4.8%. However, the system design changes more substantially as the capacity of the slow SUSD cracker is between 15.5 and 20.0% smaller than the crackers

https://doi.org/10.1021/acs.iecr.3c02226
Ind. Eng. Chem. Res. 2023, 62, 16360−16382

with the fast interruptible operation mode. These findings highlight the importance of including the SUSD time in the modeling of chemical processes with slow SUSDs, as it plays a crucial role in determining the plant's optimal capacity and performance. Finally, the optimal cracker and ethylene storage capacities for the systems including a warm standby power and slow SUSDs can be found in Table S4 of the Supporting Information.

The findings of the cost-optimization analysis are summarized in Figure 14a–b, which show the specific cost of ethylene, excluding and including the feedstock cost, respectively. In Figure 14b, the costs are multiplied with an allocation factor to allocate the costs over the coproducts (the reader is referred to the Supporting Information for a more detailed description) and the average European ethylene price in 2019 is included for reference. The key findings are as follows (limits are discussed later):

- According to our work, the annual electricity consumption of an electric cracker with a capacity of 1000 kt ethylene per year, which is around a quarter of the ethylene production capacity in The Netherlands,[64] is equal to 4.88 TWh. Fully electrifying the currently operating crackers in The Netherlands would therefore require almost 20 TWh of (green) electricity per year, which is equal to 17.4% of the current Dutch electricity consumption.[65] This clearly shows one of the main bottlenecks in electrification.
- For the specific investment cost of the electric cracker similar to that of the conventional cracker, the production cost difference between the BAU and EC-G systems is mainly caused by the mean electricity price. However, the optimal plant capacity is mostly dependent on the standard deviation. For electricity prices with a low mean and high standard deviation, EC-G can be competitive with BAU.
- The importance of flexibility is most evident when co-optimizing the cracker with the capacities and operation of renewables and electricity storage. Maximum cost savings of 57.9% compared to an inflexible system can be achieved despite a plant capacity that is 102% larger than the reference capacity, indicating that the savings result from the smaller battery, offshore wind, and PV capacity that is required when operating the plant flexibly. Of course, these numbers are affected by large uncertainties, starting from the cracker CAPEX (both BAU and electric).
- Even though cost savings resulting from flexibility are minimal in the EC-G and EC-B systems, substantial differences in optimal plant capacity are observed.
- The OE has the most significant effect on the ethylene production cost in each of the three investigated cases, resulting in cost savings of 5.3, 4.8, and 57.9% for the EC-G, EC-B, and EC-RES systems, respectively. However, when the feedstock cost is included, the cost savings decrease to 1.3, 1.2, and 26.5% for the EC-G, EC-B, and EC-RES systems, respectively.

Emission Optimization. The transition to electric crackers is driven by the goal of reducing CO_2 emissions. However, the actual decrease in emissions depends on multiple factors, such as the source of electricity, utilization, and end-of-life of the products. For instance, if the carbon-based fuel gas from electric cracking is combusted and released to the atmosphere elsewhere, it will result in a reduced abatement, or even an increase of CO_2 emissions with respect to BAU, even when nearly 100% of the electricity is generated by renewables. This study focuses on the electric cracker flexibility potential, and we assume that additional products will be managed so as to maximize the CO_2 abatement potential. Therefore, it simplifies the environmental analysis of the process by solely focusing on the decarbonization of the heat provision in terms of direct and indirect CO_2 emissions and ignores product-related emissions along the value chain. In this section, we explore in more detail the CO_2 abatement potential of electric crackers when operating flexibly or not flexibly. First, we compared the CO_2 emissions of an inflexible electric plant with those of a conventional plant, considering various projected CO_2 intensities of the electricity grid. The reduction potential of electric cracking is defined as the decrease in emissions when switching from conventional to electric cracking while considering the same (future) carbon intensity for both cases (thereby excluding the emission reductions attributed to the decreased CO_2 intensity of the electricity grid itself). The results are listed in Table 6.

Table 6. Average Projected CO_2 Intensities and Share of Renewables of the Dutch Electricity Grid Based on the Literature[56] and the Corresponding Reduction Potentials Resulting from Inflexible Electric Cracking

year	average CO_2 intensity [kg CO_2/kWh]	share of renewables [%]	reduction potential for electric cracking [%]
2019	0.371	22.0	0.0
2025	0.208	54.7	2.6
2030	0.091	72.0	56.4
2040–2050	0.000	100.0	100.0

Not surprisingly, the extent of emission reduction through electrification of the ethylene production process is closely correlated to the CO_2 intensity of electricity. For a CO_2 intensity of 0.371 kg CO_2/kWh, which is similar to current EU values, there is no benefit in using electric cracking, from either a cost or an emissions perspective. Even with over 50% renewable electricity in the grid, the reduction potential of electric cracking with respect to BAU is minimal, at 2.6%. For context, the emissions of the BAU system would have been decreased by 3.2% due to the lower CO_2 intensity of the electricity grid in 2025 compared to 2019, despite its relatively small electricity import from the grid (it is important to note that conventional cracking typically consumes process gases for electricity generation within battery limits). A more substantial reduction in emissions (56.4%) is expected from 2030 when the projected average CO_2 intensity will fall below 0.091 kg CO_2/kWh. Although the reduction potential is still modest considering the investment required, it should be noted that the energy-related emissions of crackers might be challenging to mitigate through other means. The full realization of the CO_2 reduction potential is achieved only at CO_2 intensity close to zero, i.e., in 2040–2050.

In the previous section, we investigated the potential of flexible operation of ethylene crackers by looking at cost-minimization opportunities. However, given that electric crackers are justified only as a means to decrease emissions, it is legitimate to ask if a flexible operation should follow the CO_2 intensity of the grid rather than the electricity price.

https://doi.org/10.1021/acs.iecr.3c02226
Ind. Eng. Chem. Res. 2023, 62, 16360–16382

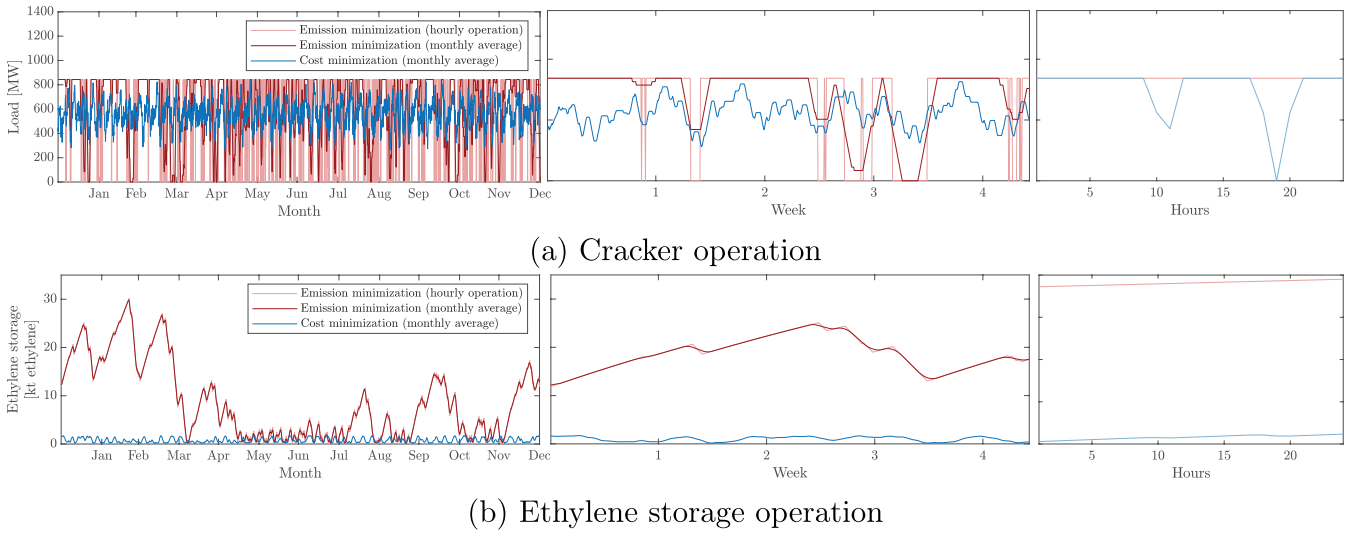

Figure 15. Cracker and ethylene storage operation for the cost (blue) and emission (red) optimizations of the full year, the first month, and the first day of the second week (left to right). For the emission optimization, the 2030 CO_2 intensity profile is used. The darker blue and red lines in the full year and first month of operation represent the moving averages of the cost and emission optimizations, respectively.

Therefore, we evaluated the potential for further reduction of CO_2 emissions through the use of flexible electric cracking for ethylene production, when flexibility is adopted to respond to varying CO_2 intensities to minimize emissions. In order to avoid unrealistic plant capacity, where, for example, the total annual ethylene demand is produced within a single hour with no CO_2 emissions, we have fixed the capacity of the EC at the cost-optimal level for a fully flexible cracker exploiting fluctuating electricity prices (which is found to be 53% higher than the inflexible reference capacity). It is worth noting that adding costs with low weight in the CO_2 objective function might have led to slightly different capacities; however, these differences are negligible for the scope of this work and the uncertainties in the cost functions.

We run this operation optimization taking into account the CO_2 intensity profiles for the years 2019 and 2030. Our analysis of the 2019 CO_2 intensity profile shows that while there is still no benefit in using electric cracking (compared to the BAU system), the emissions of flexible electric cracking are 3.0% lower than those generated by the inflexible operation. Furthermore, in 2030, the emission reduction potential of electric cracking will increase from 56.4 to 90.4% when flexible operation is optimized for CO_2 emissions. Figure 15 shows the operation of the cracker and ethylene tank of the emission minimization in comparison with the fully flexible EC-G operation profiles of the cost minimization in the previous section. Notably, the higher offshore wind electricity generation during winter months contributes to a relatively lower grid CO_2 intensity. As a result, the cracker is more frequently operated at maximum capacity during this period, consequently leading to an increase in the product inventory within the ethylene storage tank. While in the case of emission minimization clear seasonal variations are present, the cost minimization of the EC-G system mostly results in daily or weekly variations.

It is important to note that the associated cost savings potential of these emission reductions depends on how well the electricity prices reflect the availability of renewable electricity on the grid. In this study, the 2030 CO_2 intensity profile and the modified price profile are completely independent. As a result, we did not identify the potential cost reduction associated with emitting less CO_2. In fact, for future electricity prices and CO_2 intensities, the optimization of operations based on emissions leads to an increase in total annual costs by 25%. However, with improved alignment between electricity prices and low-carbon electricity, flexible operation of the ethylene production process could lead to simultaneous reductions in costs and emissions. In summary, the findings of the environmental analysis are in line with or even extend the prior findings of the economic analysis and emphasize the critical role of flexibility in enabling cost-effective decarbonization of the ethylene production process via electric crackers.

DISCUSSION

As for all models, limitations in this work exist, which we highlight here. We can first recognize that two main categories of limitations are present in this work: one associated with simplifications of physical reality in the model and one associated with uncertainties in input parameters.

Simplifications. Due to the highly complex and nonlinear nature of the ethylene production process, several simplifications were necessary in the synthesis of a MILP model. First, it should be noted that the aim of this work is to provide a top-down evaluation of the flexibility potential of the process within a larger (energy) system as opposed to investigating the specific reactor design, operation, and control that enables flexible operation. Therefore, we approximate nonlinear behavior by (piecewise) linear formulations for the three main sections of the ethylene production plant, even though in reality multiple processes exist within the sections. As the flexible operation of a cracker requires a larger reactor or multiple units, we note that the design of the control may present additional challenges that should be considered. Moreover, we consider plant dynamics to be controlled by the pyrolysis unit, which is also the most technically challenging. However, for modular and fast pyrolysis design, the separation section might become the slowest section, thus controlling the flexible operation of the plant. In this case, once there is a deeper understanding of the electric cracker, the

https://doi.org/10.1021/acs.iecr.3c02226
Ind. Eng. Chem. Res. 2023, 62, 16360−16382

separation section can also be redesigned to allow for flexibility in the operation. Additionally, while we investigate three key flexibility parameters, a more comprehensive analysis of the process dynamics is required to deepen our understanding of a flexible cracker operation. Each of these considerations requires detailed (nonlinear) models, which would introduce a level of complexity that would hinder the temporal and spatial resolution we have included in this study. Hence, our model of the electric ethylene production process aims to complement reactor-level investigations by providing guidelines on the role of flexibility. The next step would call for bridging specific reactor design with MILP-based optimization, for which the model provided here can be used with updated specific technology parameters.

Second, our analysis is location agnostic, while in reality location- or network-based limitations might play a role in the capital expenses, product use and prices, deployment of renewable and energy storage technologies, and (their effect on) electricity prices and CO_2 intensities. For example, network connections, energy transport costs, and area constraints were excluded from the optimization. While this is not expected to substantially affect the optimal capacity and flexibility potential, which is the main aim of this work, certain locations might have additional constraints for the system.

Finally, the decoking procedure was neglected, potentially underestimating investment and operating costs, energy consumption, and emissions. On the contrary, a conservative approach was used for the estimation of other parameters that affect cost and emissions, such as the assumption that the fuel consists only of methane.

Assumptions. As a result of the lack of available and reliable cost and performance data for the technologies and the highly specific nature of ethylene production plants, a set of uncertain assumptions was made in this study. For example, due to the low technology readiness level of electric cracking, the reactor design and consequences for the rest of the plant design are uncertain. Consequently, the energy and material balance of the plant may be different from the values obtained in this study, possibly affecting the absolute cost and emission reduction potential of flexible cracker operation. Nevertheless, we do not expect this to substantially change the comparative conclusions among the different cases investigated. Furthermore, the assumptions made on future hourly electricity prices and grid emission profiles are inherently highly uncertain. Additionally, cost and performance parameters of the ethylene production process were collected and computed top-down (e.g., based on average reported values). The analysis in Figure 7 shows the sensitivity of the results toward these inputs. As they strongly determine the potential of flexible operation, this should be considered in the interpretation of the results.

We emphasize that improving each of the limitations mentioned in the discussion could be targeted in future work. A logical starting point would be addressing the uncertainties in the design, performance, and CAPEX of the electric cracker.

CONCLUSIONS

In this work, we developed an efficient MILP model of conventional and electric ethylene production plants that describes the underlying key processes starting from energy and mass balances of the system. The model allows for co-optimization of capacity and operation and is therefore suitable for modeling the transition of larger industrial clusters or energy systems. We used the model to investigate the impact of flexibility in electric crackers on costs and CO_2 emissions, optimizing electric cracker capacity and operation in three scenarios (importing grid electricity with/without battery storage or co-designing renewable electricity generation). For each of these systems, we compared ethylene production costs and optimal plant size, considering different operating modes and flexibility parameters such as the operating envelope, the ramping time, and the start-up and shut-down time. Additionally, we optimized electric cracker flexibility to mitigate CO_2 emissions by following a fluctuating grid CO_2 intensity.

Our results show that for an inflexible EC with the same capacity as conventional processes, 70.6% of the ethylene production cost (excluding naphtha feedstock) can be allocated to electricity consumption, compared to 9.2% for the BAU system. As a result, the production costs decrease when flexible operation is possible (e.g., by 5.5% for the future baseline profile); however, this is highly dependent on electricity prices. Our sensitivity analysis showed that the cost of ethylene from electric crackers is mainly dependent on the mean electricity price, while the cracker's nominal capacity is mostly affected by the standard deviation. Moreover, for price profiles with a low yearly average (<25 €/MWh) and a high yearly standard deviation (>40 €/MWh), flexible electric cracking might become cost-competitive with the conventional production process. However, this can only be achieved by optimizing the cracker capacity based on the operation, leading to a larger installed capacity, lower utilization factors, and flexibility in the operation of the plant.

Furthermore, we investigated smaller operating envelopes and constrained ramping time for crackers that import electricity from the grid and found that both factors have a small effect (maximum 5.5 and 0.4% difference with inflexible operation, respectively) on the production cost. However, the relatively small cost difference is achieved if, and only if, the plant capacity is optimized for each parameter combination. Allowing for interruptible operation of electric crackers can decrease cost by up to 4.8%; however, such an operation poses challenges due to the large temperature fluctuations. Hence, we assessed the impact of including a warm standby, which can potentially facilitate fast interruptible operation by using electricity to maintain the cracker at a high temperature during shut-downs. We found that including the warm standby power in the model has a negligible effect on the production cost (<1%) and a minimal effect on the installed capacity (<6%). Finally, including slower start-ups and shut-downs (up to 6 h) leads to a maximum 4.8% cost increase compared to fast interruptible operation, while the capacity of the plant decreases by 15.5−20.0%. Likely, adding the constraints for the warm standby and longer startups and shutdowns improves the model representation of physical reality, in case of longer startups and shutdowns at the cost of a more complex resolution.

When analyzing the electric cracker systems including renewables, we find that the operating envelope has a significant effect on the production cost (57.9% difference between flexible and inflexible operation), while the effect of the ramping time is again minimal. This increased cost for limited flexibility is caused by the higher battery and renewable capacity that is required to deal with fluctuations in the supply; for example, the installed battery capacity increased from 500 MWh to 37.4 GWh between a flexible and inflexible plant capacity. Furthermore, as fully electrifying the currently

https://doi.org/10.1021/acs.iecr.3c02226
Ind. Eng. Chem. Res. 2023, 62, 16360−16382

operating crackers in The Netherlands would require almost 20 TWh of green electricity per year, flexible cracker operation can increase the feasibility with respect to grid instability and renewables and battery capacity.

Finally, our results show that the emission reduction potential of inflexible electric cracking is closely correlated with the CO_2 intensity of the electricity, resulting in a small potential reduction of 2.6% in 2025 to a 56.4% reduction in 2030. However, operating a plant flexibly in response to fluctuating hourly CO_2 intensities can increase the 2030 potential to 90.4% and, provided that CO_2 intensities are reflected in the electricity price, could reduce the production cost simultaneously. In summary, our results clearly reveal the importance of (i) including the plant capacity in the optimization problem and (ii) considering the capacity and operation of renewables and energy storage in the adoption of electric ethylene production to avoid unrealistic capacity. Moreover, we highlight that flexible electric cracker operation makes the adoption of electric crackers more cost- and emission-effective at both a plant level and energy system level.

■ ASSOCIATED CONTENT

Supporting Information

The Supporting Information is available free of charge at https://pubs.acs.org/doi/10.1021/acs.iecr.3c02226.

Additional information regarding the generation of electricity price and CO_2 intensity profiles, the optimal capacities and simulation times of all the analyzed systems, and the calculation of the coproduct cost allocation factor. One 8760-h example results file of the EC-G system for the noninterruptible operation mode with an operating envelope of 40% and a ramping time of 8 h (PDF)

■ AUTHOR INFORMATION

Corresponding Author

Matteo Gazzani − *Copernicus Institute of Sustainable Development, Utrecht University, Utrecht 3584 CB, Netherlands; Sustainable Process Engineering Chemical Engineering and Chemistry, Eindhoven University of Technology, Eindhoven 5612 AP, Netherlands;* orcid.org/0000-0002-1352-4562; Email: m.gazzani@uu.nl

Authors

Julia L. Tiggeloven − *Copernicus Institute of Sustainable Development, Utrecht University, Utrecht 3584 CB, Netherlands; TNO, Energy Transition Studies, Amsterdam 1030 CE, Netherlands*

André P. C. Faaij − *Copernicus Institute of Sustainable Development, Utrecht University, Utrecht 3584 CB, Netherlands; TNO, Energy Transition Studies, Amsterdam 1030 CE, Netherlands*

Gert Jan Kramer − *Copernicus Institute of Sustainable Development, Utrecht University, Utrecht 3584 CB, Netherlands*

Complete contact information is available at: https://pubs.acs.org/10.1021/acs.iecr.3c02226

Notes

The authors declare no competing financial interest.

■ LIST OF ABBREVIATIONS

CAPEX	capital cost
BAU	business as usual
BEC	bare erected cost
CCAF	coproduct cost allocation factor
COCF	contingencies and owner's cost factor
DSM	demand side management
EC	electric cracker
EC-G	electric cracker-grid
EC-B	electric cracker-battery
EC-RES	electric cracker-renewables
HP	high pressure
ICF	indirect cost factor
IF	installation factor
LCOEt	levelized cost of ethylene
MES	multienergy system
MILP	mixed-integer linear programming
MIP	mixed-integer programming
OE	operating envelope
OPEX	operating expenditures
PV	photovoltaics
RT	ramping time
SEC	specific energy consumption
SUSD	start-up and shut-down
TOC	total overnight cost
TD	minimum downtime
WSP	warm standby power

■ LIST OF MATHEMATICAL SYMBOLS

Indices

$j \in \mathcal{J}$	set of coproducts
$m \in \mathcal{M}$	set of technologies
$n \in \mathcal{N}$	set of carriers
$n' \in \mathcal{N}'$	subset of plant output carriers
$n'' \in \mathcal{N}''$	subset of plant input carriers
$t \in T$	set of timesteps

Variables

A	constraint matrix continuous variable
B	constraint matrix binary variable
D	carrier demand
E^{SUSD}	plant input during start-up/shut-down
F	consumption of technology
I	carrier import
J	total system cost
K	total system emission
P	production of technology
S	technology size
X	carrier export
b	constraint know term
c	cost vector for continuous variable
d	cost vector for binary variable
v	continuous variable
w	binary variable
x	binary on/off status plant
y	binary start-up plant
z	binary shut-down plant

Parameters

α	conversion efficiency plant
β	input ratio plant
γ	minimum feasible load point
ε	emission factor

https://doi.org/10.1021/acs.iecr.3c02226
Ind. Eng. Chem. Res. 2023, 62, 16360−16382

ζ size-independent cost parameter
η coproduct yield
λ size-dependent cost parameter
ν import price
ϕ warm standby power fraction
τ start-up and shut-down time
ψ maintenance cost fraction
ω annuity factor

REFERENCES

(1) IPCC. *Climate Change 2022: Impacts, Adaptation and Vulnerability*; Summary for Policymakers; Cambridge University Press: UK and New York, USA, 2022; pp 3−33.
(2) Gabrielli, P.; Rosa, L.; Gazzani, M.; Meys, R.; Bardow, A.; Mazzotti, M.; Sansavini, G. Net-zero emissions chemical industry in a world of limited resources. *One Earth* **2023**, *6*, 682−704.
(3) Ren, T.; Patel, M.; Blok, K. Olefins from conventional and heavy feedstocks: Energy use in steam cracking and alternative processes. *Energy* **2006**, *31*, 425−451.
(4) Ren, T.; Patel, M. K.; Blok, K. Steam cracking and methane to olefins: Energy use, CO2 emissions and production costs. *Energy* **2008**, *33*, 817−833.
(5) Amghizar, I.; Dedeyne, J. N.; Brown, D. J.; Marin, G. B.; Geem, K. M. V. Sustainable innovations in steam cracking: Co2 neutral olefin production. *React. Chem. Eng.* **2020**, *5*, 239−257.
(6) Zhang, Q.; Grossmann, I. E. Enterprise-wide optimization for industrial demand side management: Fundamentals, advances, and perspectives. *Chem. Eng. Res. Des.* **2016**, *116*, 114−131.
(7) Golmohamadi, H. Demand-side management in industrial sector: A review of heavy industries. *Renewable Sustainable Energy Rev.* **2022**, *156*, 111963.
(8) Riese, J.; Grunewald, M. Challenges and Opportunities to Enhance Flexibility in Design and Operation of Chemical Processes. *Chem. Ing. Technol.* **2020**, *92*, 1887−1897.
(9) Helin, K.; Käki, A.; Zakeri, B.; Zakeri, B.; Lahdelma, R.; Lahdelma, R.; Syri, S. Economic potential of industrial demand side management in pulp and paper industry. *Energy* **2017**, *141*, 1681−1694.
(10) Herre, L.; Tomasini, F.; Paridari, K.; Söder, L.; Nordström, L. Simplified model of integrated paper mill for optimal bidding in energy and reserve markets. *Appl. Energy* **2020**, *279*, 115857.
(11) Halmschlager, V.; Birkelbach, F.; Hofmann, R. Optimizing the utilization of excess heat for district heating in a chipboard production plant. *Case Stud. Therm. Eng.* **2021**, *25*, 100900.
(12) Seo, K.; Edgar, T. F.; Baldea, M. Optimal demand response operation of electric boosting glass furnaces. *Appl. Energy* **2020**, *269*, 115077.
(13) Mitra, S.; Grossmann, I. E.; Pinto, J. M.; Arora, N. Optimal Production Planning under Time-sensitive Electricity Prices for Continuous Power-intensive Processes. *Comput. Chem. Eng.* **2012**, *38*, 171−184.
(14) Gerami, N.; Ghasemi, A.; Lotfi, A.; Kaigutha, L. G.; Marzband, M. Energy consumption modeling of production process for industrial factories in a day ahead scheduling with demand response. *Sustainable Energy Grids Netw.* **2021**, *25*, 100−420.
(15) Zhang, X.; Hug, G.; Harjunkoski, I. Cost-Effective Scheduling of Steel Plants with Flexible EAFs. *IEEE Trans. Smart Grid* **2017**, *8*, 239−249.
(16) Tan, M.; Yang, H. L.; Duan, B.; Su, Y. X.; He, F. Optimizing Production Scheduling of Steel Plate Hot Rolling for Economic Load Dispatch under Time-of-Use Electricity Pricing. *Math. Probl. Eng.* **2017**, *2017*, No. 1048081, DOI: 10.1155/2017/1048081.
(17) Ramin, D.; Spinelli, S.; Brusaferri, A. Demand-side management via optimal production scheduling in power-intensive industries: The case of metal casting process. *Appl. Energy* **2018**, *225*, 622−636.
(18) Lahrsen, I. M.; Hofmann, M.; Müller, R. Flexibility of Epichlorohydrin Production - Increasing Profitability by Demand Response for Electricity and Balancing Market. *Processes* **2022**, *10*, 761.
(19) Otashu, J. I.; Baldea, M. Demand response-oriented dynamic modeling and operational optimization of membrane-based chlor-alkali plants. *Comput. Chem. Eng.* **2019**, *121*, 396−408.
(20) Hofmann, M.; Müller, R.; Christidis, A.; Fischer, P.; Klaucke, F.; Vomberg, S.; Tsatsaronis, G. Flexible and economical operation of chlor-alkali process with subsequent polyvinyl chloride production. *AIChE J.* **2022**, *68*, No. e17480.
(21) Ierapetritou, M. G.; Wu, D.; Vin, J.; Sweeney, P.; Chigirinskiy, M. Cost minimization in an energy-intensive plant using mathematical programming approaches. *Ind. Eng. Chem. Res.* **2002**, *41*, 5262−5277.
(22) Kelley, M. T.; Pattison, R. C.; Baldick, R.; Baldea, M. An MILP framework for optimizing demand response operation of air separation units. *Appl. Energy* **2018**, *222*, 951−966.
(23) Basán, N. P.; Grossmann, I. E.; Gopalakrishnan, A.; Lotero, I.; Méndez, C. A. Novel MILP Scheduling Model for Power-Intensive Processes under Time-Sensitive Electricity Prices. *Ind. Eng. Chem. Res.* **2018**, *57*, 1581−1592.
(24) Xenos, D. P.; Noor, I. M.; Matloubi, M.; Cicciotti, M.; Haugen, T.; Thornhill, N. F. Demand-side management and optimal operation of industrial electricity consumers: An example of an energy-intensive chemical plant. *Appl. Energy* **2016**, *182*, 418−433.
(25) Cao, Y.; Swartz, C. L.; Flores-Cerrillo, J. Optimal Dynamic Operation of a High-Purity Air Separation Plant under Varying Market Conditions. *Ind. Eng. Chem. Res.* **2016**, *55*, 9956−9970.
(26) Miller, J.; Luyben, W. L.; Blouin, S. Economic incentive for intermittent operation of air separation plants with variable power costs. *Ind. Eng. Chem. Res.* **2008**, *47*, 1132−1139.
(27) Mitra, S.; Pinto, J. M.; Grossmann, I. E. Optimal Multi-scale Capacity Planning for Power-Intensive Continuous Processes under Time-sensitive Electricity Prices and Demand Uncertainty, Part I: Modeling. *Comput. Chem. Eng.* **2014**, *65*, 89−101.
(28) Roh, K.; Brée, L. C.; Perrey, K.; Bulan, A.; Mitsos, A. Flexible operation of switchable chlor-alkali electrolysis for demand side management. *Appl. Energy* **2019**, *255*, No. 113880.
(29) Teichgraeber, H.; Brodrick, P. G.; Brandt, A. R. Optimal design and operations of a flexible oxyfuel natural gas plant. *Energy* **2017**, *141*, 506−518.
(30) Teichgraeber, H.; Brandt, A. R. Optimal design of an electricity-intensive industrial facility subject to electricity price uncertainty: Stochastic optimization and scenario reduction. *Chem. Eng. Res. Des.* **2020**, *163*, 204−216.
(31) Zimmermann, H.; Walzi, R. *Ullmann's Encyclopedia of Industrial Chemistry*; John Wiley & Sons, Ltd, 2009.
(32) Tuomaala, M.; Hurme, M.; Leino, A. M. Evaluating the efficiency of integrated systems in the process industry-Case: Steam cracker. *Appl. Therm. Eng.* **2010**, *30*, 45−52.
(33) Falcke, H.; Holbrook, S.; Clenahan, I.; Carretero, A. L.; Sanalan, A.; Brinkmann, T.; Roth, J.; Zerger, B.; Roudier, S.; Sancho, L. D. *Best Available Techniques (BAT) Reference Document for the Production of Large Vol. Organic Chemicals. Industrial Emissions Directive 2010/75/EU (Integrated Pollution Prevention and Control)*; Publications Office of the European Union: Luxembourg, 2017; p JRC109279.
(34) Yang, M.; You, F. Comparative Techno-economic and Environmental Analysis of Ethylene and Propylene Manufacturing from Wet Shale Gas and Naphtha. *Ind. Eng. Chem. Res.* **2017**, *56*, 4038−4051.
(35) Spallina, V.; Velarde, I. C.; Jimenez, J. A. M.; Godini, H. R.; Gallucci, F.; Annaland, M. V. S. Techno-economic assessment of different routes for olefins production through the oxidative coupling of methane (OCM): Advances in benchmark technologies. *Energy Convers. Manage.* **2017**, *154*, 244−261.
(36) DEA. Technology Data-Industrial Process Heat, 2020. https://ens.dk/sites/ens.dk/files/Analyser/technology_data_catalogue_for_industrial_process_heat.pdf (accessed Nov 14, 2022).
(37) Tan, H.; Cai, W.; Wang, Q. G.; Sun, N. In *Optimization and Comparison of Boiling-Off Gas Re-Liquefaction Processes for Liquid*

Ethylene Vessels, Proceedings of the 2016 IEEE 11th Conference on Industrial Electronics and Applications, 2016; pp 717−722.
(38) Yafei, J. Z. Z. J. W. Method for Liquid Phase Ethylene Storage by Combination of Ordinary Pressure and Medium Pressure. CN Patent CN1542319A2003.
(39) Edwin, E. H.; Balchen, J. G. Dynamic optimization and production planning of thermal cracking operation. *Chem. Eng. Sci.* **2001**, *56*, 989−997.
(40) Wong, L.; Dril, A. W. N. V. Decarbonisation Options for Large Volume Organic Chemicals Production; Shell Moerdijk, 2020. https://www.pbl.nl/en/publications/decarbonisation-options-for-large-volume-organic-chemicals-production-shell-moerdijk (accessed Jan 17, 2023).
(41) Oliveira, C.; Dril, A. W. N. Decarbonisation Options for Large Volume Organic Chemicals Production; SABIC Geleen, 2021. https://www.pbl.nl/en/publications/decarbonisation-options-for-large-volume-organic-chemicals-production-sabic-geleen (accessed Jan 17, 2023).
(42) Tullo, A. S. *Dow Test Electric Cracking*; C&EN Global Enterprise, 2022; Vol. *100*, p 12.
(43) Tullo, A. *BASF, Sabic, and Linde to Test Electric Cracker*; C&EN Global Enterprise, 2022; Vol. *100*, p 8.
(44) Balakotaiah, V.; Ratnakar, R. R. Modular reactors with electrical resistance heating for hydrocarbon cracking and other endothermic reactions. *AIChE J.* **2022**, *68*, No. e17542.
(45) Ghashghaee, M.; Karimzadeh, R. Multivariable optimization of thermal cracking severity. *Chem. Eng. Res. Des.* **2011**, *89*, 1067−1077.
(46) Gabrielli, P.; Gazzani, M.; Mazzotti, M. Electrochemical conversion technologies for optimal design of decentralized multi-energy systems: Modeling framework and technology assessment. *Appl. Energy* **2018**, *221*, 557−575.
(47) Gabrielli, P.; Gazzani, M.; Martelli, E.; Mazzotti, M. Optimal design of multi-energy systems with seasonal storage. *Appl. Energy* **2018**, *219*, 408−424.
(48) Weimann, L.; Gabrielli, P.; Boldrini, A.; Kramer, G. J.; Gazzani, M. Optimal hydrogen production in a wind-dominated zero-emission energy system. *Adv. Appl. Energy* **2021**, *3*, No. 100032.
(49) Geidl, M.; Koeppel, G.; Favre-Perrod, P.; Klöckl, B.; Andersson, G.; Fröhlich, K. In *Energy Hub-A Powerful Concept for Future Energy Systems*, Third Annual Carnegie Mellon Conference on the Electricity Industry, 2007; pp 13−14.
(50) The MathWorks Inc. MATLAB, version 9.4 (R2018a), 2018. https://www.mathworks.com/products/matlab.html (accessed Jun 9, 2023).
(51) Löfberg, J. In *YALMIP: A Toolbox for Modeling and Optimization in MATLAB*, Proceedings of the 2004 IEEE International Conference on Robotics and Automation (IEEE Catal. No. 04CH37508), 2004; pp 284−289.
(52) Gurobi Optimization LLC. Gurobi, version 9.1, 2000. http://www.gurobi.com (accessed Jun 9, 2023).
(53) Kwon, H.; Do, T. N.; Won, W.; Kim, J. An optimization model for the market-responsive operation of naphtha cracking process with price prediction. *Chem. Eng. Res. Des.* **2022**, *188*, 681−693.
(54) Morales-España, G.; Ramírez-Elizondo, L.; Hobbs, B. F. Hidden power system inflexibilities imposed by traditional unit commitment formulations. *Appl. Energy* **2017**, *191*, 223−238.
(55) ENTSO-E. Day-Ahead Prices and Hourly Generation Per Production Type for the Netherlands in 2019, 2019. https://transparency.entsoe.eu/dashboard/show (accessed Jan 9, 2023).
(56) van Cappellen, L.; Wielders, L.; Scholten, T. Emissiefactor elektriciteit uit fossiele bronnen-Voor compensatieregeling IKC-ETS, 2021. https://www.rvo.nl/sites/default/files/2022-05/CE_Delft_210338_Emissiefactor_Elektriciteit_Fossiele_Bronnen_DEF.pdf (accessed Jan 9, 2023).
(57) Royal Netherlands Meteorological Institute (KNMI). Climate Data, 2019. https://climexp.knmi.nl (accessed Jan 9, 2023).
(58) Royal Netherlands Meteorological Institute (KNMI). Dutch Offshore Wind Atlas (DOWA) Data, 2019. https://www.dutchoffshorewindatlas.nl/about-the-atlas/dowa-data/data-downloads (accessed Jan 9, 2023).
(59) Navigant Consulting. Verkenning uitbreiding SDE + met industriële opties, 2019. https://open.overheid.nl/documenten/ronl-09648079-1236-4447-a528-b1ebeba329c1/pdf (accessed Jan 17, 2023).
(60) Turton, R.; Bailie, R. C.; Whiting, W. B.; Shaeiwitz, J. A. *Analysis, Synthesis and Design of Chemical Processes*; Pearson Education, 2008.
(61) DEA. Technology Data-Energy Plants for Electricity and District Heating Generation, 2022. http://www.ens.dk/teknologikatalog (accessed Nov 14, 2023).
(62) DEA. Technology Data-Energy Storage, 2022. http://www.ens.dk/teknologikatalog (accessed Nov 14, 2023).
(63) Theis, J. *Cost Estimation Methodology for NETL Assessments of Power Plant Performance*; National Energy Technology Laboratory (NETL), 2019.
(64) Petrochemicals Europe. Cracker Capacity (kt ethylene/year) in Europe in 2021, 2021. https://www.petrochemistry.eu/about-petrochemistry/petrochemicals-facts-and-figures/cracker-capacity/ (accessed Aug 22, 2023).
(65) CBS. Electricity Balance Sheet Supply and Consumption, 2019. https://opendata.cbs.nl/#/CBS/en/dataset/84575ENG/table (accessed Aug 22, 2023).
(66) IEA. Annual Ethylene Capacity/Demand Growth and Regional Price Developments, 2015−2020, 2019. https://www.iea.org/data-and-statistics/charts/annual-ethylene-capacity-demand-growth-and-regional-price-developments-2015-2020 (accessed Sep 6, 2023).

https://doi.org/10.1021/acs.iecr.3c02226
Ind. Eng. Chem. Res. 2023, 62, 16360−16382